Final Project Report

Examining the Abrasion and Carbonation Resistance of Portland Limestone Cement (PLC) Systems for Industrial Floors

ACI Foundation

Concrete Advancement Foundation

American Cement Association

Mehdi Khanzadeh Moradllo, Ph.D., P.E. (Principal Investigator)

Syed Jafar Shah Bukhari, Ph.D. Student

Ifeanyi Onuoha, Ph.D. Student

Armin Hajihassani, B.Sc. Student

Temple University

Philadelphia, Pennsylvania

March 2026

Acknowledgments

The authors gratefully acknowledge the financial support from the American Concrete Institute Foundation, the Concrete Advancement Foundation, and the Portland Cement Association Foundation through the J.P. Gleason Research Fellowship. We are also thankful to Concrete Strategies LLC, specifically Mr. Kyle Kammer and Mr. Sam Klucker, for their collaboration and assistance in conducting field experiments. The authors are grateful to Dr. Claire Nowasell of Heidelberg Materials for assistance in conducting XRD and XRF experiments.

Disclaimer

The contents of this report reflect the views of the authors who are responsible for the facts and accuracy of the data presented herein. The contents do not necessarily reflect the official views of the funding organizations at the time of publication. This report does not constitute a standard, specification, or regulation.

Project Executive Summary

Fulfillment and distribution centers are becoming a sizable concrete construction sector. As society navigates post-pandemic, many online retailers are expecting to increase their physical footprint. At the same time, to respond to the threat of climate change, concrete industry is looking for approaches to reduce embodied carbon. Therefore, transitioning from Ordinary Portland Cement (OPC) to Portland Limestone Cement (PLC), which has a lower embodied carbon, seems to be a logical next step. While many studies have been performed to compare the mechanical properties and permeability of PLC and OPC systems, there is a lack of research/experimental data on the abrasion resistance of PLC systems. In most cases, a fulfillment/distribution center has millions of square feet of concrete slabs that need to be durable for different types of traffic and millions of cycles. Therefore, further research is needed to systematically study the abrasion resistance of PLC systems using standard test methods.

This project addresses this need with the goal of providing the concrete industry with data to make informed decisions on the potential use of PLC systems for industrial floors. This study examines the abrasion resistance of PLC and PLC+SCM systems and compares them with those of OPC systems according to BS 8204-2 standard test method in laboratory and field settings. Additionally, the impact of fiber reinforcement and surface hardeners/densifiers on the abrasion resistance of PLC systems was examined. The objective of this study is to provide a fulfillment/distribution center with a cement system that is both durable and sustainable. This study also examines the carbonation rate of PLC systems. Early-age carbonation of concrete could cause early delamination of concrete floors.

Contents

1 Introduction

Concrete industrial floors are subjected to repeated rolling, sliding, and impact actions that progressively degrade the surface through abrasion. Abrasion resistance is therefore a critical performance parameter governing the serviceability and life-cycle cost of industrial floor systems. Considering that fulfillment and distribution centers are becoming a sizable concrete construction sector, inadequate abrasion resistance can lead to costly maintenance interventions and life-cycle costs for the industry. The North America commercial concrete flooring market size was valued at $1.6 billion in 2022 [1]. As society navigates post-pandemic, many online retailers expect to increase their physical footprint. For example, some warehouses have over 200,000 square meters of floor space at ground level (requiring approximately 35,000 cubic meters of concrete) [2, 3]. At the same time, to respond to the threat of climate change, the cement and concrete industry is looking for approaches to reduce concrete's embodied carbon. The estimated CO_2 emission per square meter of floor slab is approximately 80-120 kg-CO_2 [4]. Therefore, transitioning from ASTM C150 [5] Ordinary Portland Cement (OPC) to ASTM C595 [6] Portland Limestone Cement (PLC; i.e., Type IL cement), which has a lower embodied carbon, can be a viable strategy. PLC is designed to enable more sustainable concrete production by partially replacing cement clinker with interground limestone particles [7, 8]. The replacement of 15% of the mass of the clinker by limestone reduces CO_2 emissions on average by 12% [7, 8, 9]. However, there is limited research on the abrasion resistance of PLC systems for applications in industrial floors. Industrial concrete floors need to be durable for different types of heavy traffic and millions of cycles. Extensive wear depth in industrial concrete floors can lead to expensive repair/maintenance costs.

According to the ACI 302 Guide to Concrete Floor and Slab Construction [10], a concrete mixture for industrial floors should develop the required surface abrasion resistance, wear resistance, impact resistance, flexural strength, and shrinkage characteristics. Overall, previous research indicates that PLC can achieve comparable or even enhanced compressive strength compared to OPC, particularly at later ages (e.g., 28 days and beyond) [11, 12]. This is mainly attributed to the filler effect of the limestone, which refines the microstructure. In addition, limestone particles can serve as nucleation sites to enhance hydration and microstructure development [11]. Previous studies also suggest that PLC concrete exhibits comparable or slightly lower flexural strength and modulus of elasticity compared to OPC concrete [13]. Meddah et al. [13] reported that the slight decrease can be attributed to the fact that limestone primarily acts as a filler, which can lead to the formation of an additional weaker interfacial transition zone (ITZ) within the cement matrix. Studies have indicated that PLC concrete can exhibit comparable or improved resistance to chloride ion penetration compared to OPC concrete, which can be attributed to the filler effect of ground limestone, enhancing particle packing density and refining the microstructure [14-17].

While many studies have been performed to compare the mechanical properties and permeability of PLC and OPC systems [18-23]. There is limited research/experimental data on the abrasion resistance of PLC systems. In most cases, a fulfillment/distribution center has thousands of square meters of concrete slabs that need to be durable for different types of traffic and millions of cycles. Dhir et al. [24] investigated the abrasion resistance of concrete produced using combinations of OPC and ground limestone up to 45% replacement level. The addition of 15% ground limestone showed a minimal impact on the abrasion resistance of concrete [24]. However, by increasing the ground limestone content to 25%, the abrasion depth of OPC-limestone concrete was 35% greater than the corresponding OPC concrete. However, the study by Dhir et al. [24] used a single ground limestone source and did not examine the performance of

interground clinker/limestone system (i.e., PLC concrete). The abrasion resistance of concrete can be sensitive to the specific mineralogy and grindability of the limestone source used in PLC production. Additionally, the study did not include any statistical measure of the variability of test results. Therefore, further research is needed to systematically study the abrasion resistance of PLC systems using standard test methods for industrial floor applications.

The abrasion resistance of concrete is influenced by multiple factors, including water-to-cement ratio (w/c) [25], compressive strength [25-27], curing time and conditions [25], aggregate properties [27], surface finishing technique [27], and the incorporation of supplementary cementitious materials (SCMs) and fibers [26]. A lower w/c ratio enhances abrasion resistance by reducing porosity and increasing surface hardness [27-29]. High-compressive strength concrete generally exhibits superior abrasion resistance due to its dense microstructure, which provides better wear resistance under mechanical loads [29, 30]. Hadchiti and Carrasquillo [31] recommended 28-MPa (4000-psi) minimum compressive strength at the time of exposure to services. Proper curing (such as moist burlap curing for 7 days and curing compound applied immediately after the finishing) substantially improves surface durability, as premature drying leads to weak, porous concrete, reducing its resistance to wear [32, 33]. Sadegzadeh et al. [34] reported that the finishing technique utilized heavily impacts the abrasion resistance of concrete. According to their experiments, repeated power finishing yielded the best results by compacting the paste matrix and eliminating capillary channels at the surface. The type, size, and hardness of aggregates also play a critical role, with harder aggregates such as quartz or granite improving abrasion resistance compared to softer limestone aggregates [28, 29, 35]. Additionally, incorporating silica fume as SCM refines the concrete matrix, reducing surface degradation [28, 36, 37]. Scholz and Keshari [38] found that concrete mixtures containing a combination of silica fume and slag had superior abrasion resistance. Hadchiti and Carrasquillo [31] observed that concrete containing fly ash is as resistant to abrasion as plain concrete when compared at relatively equal strengths. Thus, optimizing these factors is essential for enhancing the durability and service life of concrete structures exposed to abrasive forces.

Several standardized methods exist globally for evaluating the abrasion resistance of concrete due to varying exposure conditions and requirements [25, 27]. ASTM C418 [39] employs a sandblasting approach, quantifying wear by measuring concrete surface loss caused by airborne abrasive particles, suited for structures facing wind-driven sand. ASTM C944 [40] involves a rotating-cutter device applying abrasion directly to the concrete surface, simulating pedestrian traffic and moderate abrasive forces. ASTM C779 [41] encompasses methods using revolving disks or steel balls, effectively mimicking heavy foot or vehicular traffic, ideal for industrial flooring applications. ASTM C1803-15 [42] uses reciprocating abrasive wheels to simulate sliding wear conditions. International standards like IS:9284–1979 (India) [43], CSA A23.2-16A/17A (Canada) [44], and GB/T16925-1997 (China) [45] provide standardized abrasion test procedures reflecting regional performance requirements. Importantly, BS EN 13892-4:2003 [46] not only evaluates abrasion resistance but also classifies concrete flooring into distinct categories based on its performance via BS 8204: Part 2: 2003 [47]. For example, based on BS 8204-2: 2003, the allowable maximum depth of wear for light-duty industrial floors (compressive strength of ≈40 MPa [5800 psi]) is 0.4 mm. Due to this practical classification system, BS EN 13892-4:2003 is widely adopted, facilitating clear specification and selection criteria for concrete flooring materials. Several studies also implemented non-destructive indirect test methods, such as initial surface absorption [48], intrinsic permeability, Schmidt rebound hammer test [48, 49], ultrasound velocity test [48, 49], 3D scanner [50], and the hardness of the concrete surface to evaluate and predict the abrasion resistance of concrete floors [28].

1.1 Organization of this Document

This report aims to provide new insights into the abrasion resistance of PLC and PLC+SCM concrete systems. The document is broken into three phases: (i) the abrasion resistance of PLC versus OPC systems considering varying sources, (ii) the abrasion resistance of binary PLC+SCM systems and impact from fiber reinforcement and surface densifiers, and (iii) the abrasion performance of PLC and PLC+SCM systems in the field.

The first phase examines the abrasion resistance of PLC systems from six different sources/producers and compares it with that of OPC systems according to BS EN 13892-4:2003. This section investigates twenty different concrete mixtures with varying w/c and binder compositions. The study also evaluates the influence of the test surface (finished surface versus formed surface) on the abrasion resistance of PLC and OPC mixtures to observe the impact of surface finishing conditions on the abrasion depth. Additionally, a surface hardener was applied to a set of samples to examine its impact on the abrasion resistance of PLC systems.

Phase 2 expands upon the phase 1 baseline by evaluating PLC concrete mixtures incorporating ground granulated blast-furnace slag (GGBFS), fly ash (FA), macro-synthetic fiber reinforcement, and lithium silicate surface densifier. All section 2 mixtures were proportioned at a fixed water-to-binder ratio (w/b) of 0.52 to represent common field mixture composition and to maximize sensitivity to mixture modifications. FA and GGBFS were used in concrete mixtures to replace 20-50% of the weight of the cementitious materials.

In phase 3, a correlation between abrasion results from the lab and field measurements was established. Three concrete mixtures with PLC in combination with slag and Class C fly ash were examined. All mixtures contained macro synthetic fibers. A lithium silicate-based surface densifier/sealer was used as a curing compound. Additionally, paste mixtures were prepared to examine the impact of lithium silicate-based curing compound on microstructure compared to sealed curing.

2 Abrasion Resistance of Portland Limestone Cement Concrete

2.1 Materials

Ordinary Portland Cement (OPC) Type I and Portland Limestone Cement (PLC) Type IL, complying with ASTM C150 [5] and ASTM C595 [6], respectively, were sourced from multiple manufacturers to ensure a comprehensive evaluation of their performance in concrete mixtures. Specifically, PLC was procured from six different sources (across the U.S.), identified as PLC1 through PLC6, to capture variations in cement properties across different production processes. OPC was obtained from source 1 (OPC1), source 4 (OPC4), and source 5 (OPC5) to compare their performance.

The X-ray diffraction (XRD) analysis revealed differences in the phase composition of OPC and PLC across the sources, as listed in Table 1. Alite (C_3S) content, a critical phase for early strength development, was notably higher in certain PLC samples (PLC5: 62.1%, PLC6: 59.33%). In contrast, belite (C_2S) content, which contributes to long-term strength, was more pronounced in PLC2 (20.5%). The high C_2S content in PLC systems may necessitate physical activation, such as higher particle fineness or chemical activation, like the use of accelerators, to compensate for slow early reaction and obtain acceptable initial strengths. As expected, the calcite and dolomite phases were more prevalent in PLC samples due to the limestone content, with PLC1 and PLC4 exhibiting over 10% calcite. The chemical composition of cement samples from various sources, as identified by X-ray fluorescence (XRF), is listed in Table 2. The XRF results align with the phase composition observed in XRD. The impact of phase variations on the performance of PLC and OPC mixtures has been discussed in the results section.

The coarse aggregate used was a crushed dolomitic limestone conforming to ASTM C33 [51] #57 gradation, with a nominal maximum aggregate size of 19 mm. The coarse aggregate possesses a specific gravity of 2.69 and an absorption capacity of 0.61%. The geological classification of the aggregate was selected to represent a standard regional material, though it is acknowledged that harder aggregates (e.g., granites, trap rock) would yield higher absolute abrasion resistance. For the fine aggregate, siliceous river sand was used with a specific gravity of 2.63, an absorption rate of 0.58%, and a fineness modulus (FM) of 2.23. To ensure the workability of the concrete mixture while maintaining the w/c, a polycarboxylate-based High-Range Water Reducer (HRWR) was incorporated. The HRWR was used to achieve and sustain a target slump of 100 ± 12.5 mm, in compliance with common workability requirements for industrial floor systems. Additionally, a commonly used water-based surface hardener (with 20-25% sodium silicate content) was utilized to evaluate its efficacy in improving the abrasion resistance of PLC systems.

Table 1—Phase Composition via Quantitative XRD for raw cement.

Phase Composition (%)	**Cement Type and Source**								
	PLC1	**PLC2**	**PLC3**	**PLC4**	**PLC5**	**PLC6**	**OPC1**	**OPC4**	**OPC5**
Alite (C_3S)	50.75	43.52	55.43	55.29	62.10	59.33	53.66	58.38	62.29
Belite (C_2S)	10.81	20.5	11.42	10.04	8.99	7.12	16.84	11.66	11.89
Calcite ($CaCO_3$)	10.49	9.31	8.87	10.46	7.88	9.22	1.03	3.93	3.21
Dolomite ($CaMg(CO_3)_2$)	1.41	2.06	0.98	1.24	0.4	0.69	1.63	1.08	0.72
Ferrite (C_4AF)	5.72	6.55	8.60	10.10	9.43	11.96	7.72	11.08	11.10
Gypsum ($CaSO_4.2H_2O$)	3.36	0.54	1.66	4.53	3.27	0.75	0.28	4.95	0.43

Table 2—Chemical composition and Phases of cements from XRF.

Chemical Composition (%)	Cement Type and Source								
	PLC1	PLC2	PLC3	PLC4	PLC5	PLC6	OPC1	OPC4	OPC5
SiO_2	18.55	19.68	19.06	18.21	19.83	18.79	19.92	19.19	20.57
Al_2O_3	5.02	4.71	3.87	4.43	3.63	4.82	5.48	4.72	4.07
Fe_2O_3	2.59	2.56	3.06	3.04	3.31	3.18	2.99	3.21	3.35
CaO	65.05	62.06	61.72	61.67	64.23	62.89	62.54	61.89	64.34
MgO	3.00	3.82	2.24	2.91	1.16	1.81	3.20	3.14	1.40
K_2O	1.10	1.04	0.80	0.46	0.35	0.66	1.17	0.53	0.39
Na_2O	0.21	0.24	0.09	0.08	0.26	0.11	0.27	0.07	0.27
SO_3	3.48	4.88	3.00	2.71	2.79	2.81	3.37	3.10	3.28
LOI	5.74	4.7	5.64	5.87	4.28	4.77	2.17	3.47	2.13
Phases (%)									
C_3S	59.26	41.83	53.55	51.86	62.74	53.67	56.01	58.35	64.46
C_2S	8.49	24.88	14.26	13.1	9.53	13.39	14.87	11.01	10.36
C_3A	8.91	8.17	5.07	6.61	4.02	7.38	9.45	7.09	5.13
C_4AF	7.88	7.78	9.32	9.24	10.07	9.68	9.11	9.77	10.19

2.2 Mixture Design

Twenty concrete mixture designs with three w/c (0.37, 0.42, and 0.52) were developed with varying dosages of HRWR based on the type and source of OPC and PLC cement to maintain the target workability of 100 mm. A w/c of 0.52 is commonly employed in industrial floor systems in the U.S. Lower w/c (0.42 and 0.37) was selected to investigate the impact of paste quality (i.e., denser matrix) on the abrasion resistance of PLC and OPC concrete. The mixture proportions are listed in Table 3 for each of the concrete mixtures. A mixture design with a w/c of 0.37 was tested for OPC1 and PLC1 cements only. Additionally, a set of PLC1 samples with a w/c of 0.52 was tested with a surface hardener applied on top after 28 days of curing using a 150 mm paint brush, followed by 24 hours of drying before testing.

Table 3—Mixture design of concrete mixtures in a saturated surface dry (SSD) condition.

Mixture	w/c	Coarse Aggregate (kg/m^3)	Fine Aggregate (kg/m^3)	Cement (kg/m^3)	Water (kg/m^3)	HRWR (g/100kg cement)
PLC1-0.52	0.52	985	849	342	178	0
PLC2 0.52						0
PLC3 0.52						0
PLC4 0.52						0
PLC5 0.52						100
PLC6 0.52						167
OPC1 0.52						0
OPC4 0.52						145
OPC5 0.52						230
PLC1 0.42	0.42	979	847	398	167	340
PLC2 0.42						380
PLC3 0.42						421
PLC4 0.42						268
PLC5 0.42						357
PLC6 0.42						375
OPC1 0.42						172
OPC4 0.42						210
OPC5 0.42						322
PLC1 0.37	0.37	1012	869	398	147	603
OPC1 0.37						587

2.3 Sample Preparation

A planetary mixer was used for the preparation of the concrete mixtures to ensure uniform distribution of materials. The coarse and fine aggregates were first combined and mixed for one minute to achieve initial homogeneity. Subsequently, cement and water, with pre-dissolved HRWR, were added to the mixture. The complete mixture was then thoroughly mixed for an additional five minutes to ensure optimal dispersion of the cementitious materials and admixture throughout the aggregate matrix.

To replicate the performance characteristics of industrial floors, rectangular prism-shaped concrete slabs measuring 525 × 512.5 × 100 mm^3 were prepared for abrasion testing, as shown in Fig. 1. The mixed concrete was poured into molds in two equal layers of 50 mm each. To achieve proper compaction, each layer was consolidated by rodding, as per ASTM C31-22 [52]. After placement, the concrete surface was first struck off using a straightedge and then lightly floated to level the surface. Final finishing was performed after the bleed water had dissipated and the surface had reached a suitable stiffness. Two consistent passes were applied using a steel hand trowel under uniform pressure to achieve a smooth and consistent surface texture. Although industrial floor slabs typically utilize power-troweling equipment, this controlled hand-troweling procedure was applied uniformly to all specimens to ensure consistency and enable comparative evaluation of surface abrasion behavior. The top (open) surface was referred to as the finished surface, while the bottom (molded) surface was referred to as the formed surface. Three replicate slab samples were made per mixture to ensure statistical reliability and repeatability in the test

results. Cylindrical samples (100 mm × 200 mm) were also prepared for compressive strength measurements.

The samples were sealed for the first 24 hours using polyethylene sheeting to limit moisture loss during early hydration. After demolding, the samples were wet cured for 14 days at 23 °C by covering both finished and formed surfaces with burlap maintained in a continuously saturated (dripping) condition. This duration of wet curing ensured continued hydration, crucial for strength development at the surface of the concrete slabs to eliminate the impact of inadequate curing on abrasion resistance. After wet curing, the samples underwent 13 days of dry air curing at a controlled temperature of 23 ± 2 °C to simulate typical drying conditions encountered by industrial floor systems. This comprehensive preparation process ensured the samples closely represented the properties and behavior of industrial floors, enabling an accurate assessment of their performance under standardized testing conditions. All the samples were tested at 28 days.

Followed by abrasion resistance testing, using a wet coring drill machine with diamond drill bits, 100 mm (diameter) cores were extracted from intact sections of slab samples for further investigation.

2.4 Accelerated Abrasion Resistance Testing

The accelerated abrasion resistance test (AART) was performed following BS EN 13892-4:2003 [46], which specifies a standardized procedure for evaluating the abrasion resistance of concrete floors. This method utilizes a specialized machine equipped with rotating hardened wheels to measure the depth of wear on the concrete surface across a designated circular area (wear path), as shown in Fig. 1. The test machine abrades the surface of concrete employing a combined rolling, sliding, and light impact action. A gearbox attached to the machine is capable of rotating the abrasion head at 180 rpm for 2,850 revolutions. BS EN 13892-4:2003 recommends an average of 8 points to measure the abrasion depth across the designated area. However, in this study, 16 points were marked equally spaced around the abrasion path using a circular template to reduce the variability of measurements. A digital depth gauge capable of measuring to the nearest 0.01mm was used to take before and after abrasion measurements. The abrasion resistance of both finished (top) and formed (bottom) surfaces was measured to quantify the impact of surface finishing conditions on the abrasion depth. It should be noted that while the formed surface is not exposed to abrasion in industrial floors, the obtained data on the formed surface (with no bleeding phenomenon and denser paste matrix) can represent a concrete floor with a good quality surface finish. AART provides a quantitative assessment of surface durability and is widely recognized in the industry for classifying abrasion resistance.

Fig. 1—(a) Untested slab sample, (b) sample during AART, and (c) sample after AART.

2.5 Compressive Strength

A compressive strength test was conducted on cylindrical samples with dimensions of 100 × 200 mm^2 after 28 days of curing, following ASTM C39-24 [53]. The samples were cured in saturated lime solution at 23 °C. The Tinius Olsen 300K Super L compression test system was used to test samples. The samples were tested at the rate of 680 kg per minute until the sample failed (i.e., reached a peak load) [54]. A minimum of three samples were tested per mixture.

2.6 Coarse Aggregate and Mortar Content at Finished/Formed Surfaces

The abrasion resistance of the finished (top) and formed (bottom) surfaces can be affected by the concentration of coarse aggregates and the quality of the paste and fine aggregates (i.e., mortar). To quantify the relative amount of coarse aggregate and mortar at finished and formed surfaces, 100-mm diameter cores were taken from intact sections of slab samples using a wet core drill machine. Then, multiple sections were cut from each core using a wet saw for imaging. After drying the sections, the coarse aggregates on each face (finished and formed surfaces) were painted with a black marker for ease in contrast-based segmentation during the image processing (Fig. 2a). High-resolution images (3024 pixels × 4032 pixels) were taken for each of the painted surfaces using a camera. The images were analyzed using ImageJ software. 5-mm slices were cropped from the finished (top) and formed (bottom) surfaces (Fig. 2b). 5-mm slice thickness was selected based on the maximum depth of abrasion from the AART. Then, a binary image was created to segment the coarse aggregate (white pixels) from the mortar part (black pixels), as shown in Fig. 2c. Finally, the area proportion of black and white pixels was calculated to quantify the percentage of mortar/coarse aggregates in the top 5 mm of the finished and formed surfaces. Eight sections were analyzed per PLC/OPC mixture, and the average results were reported.

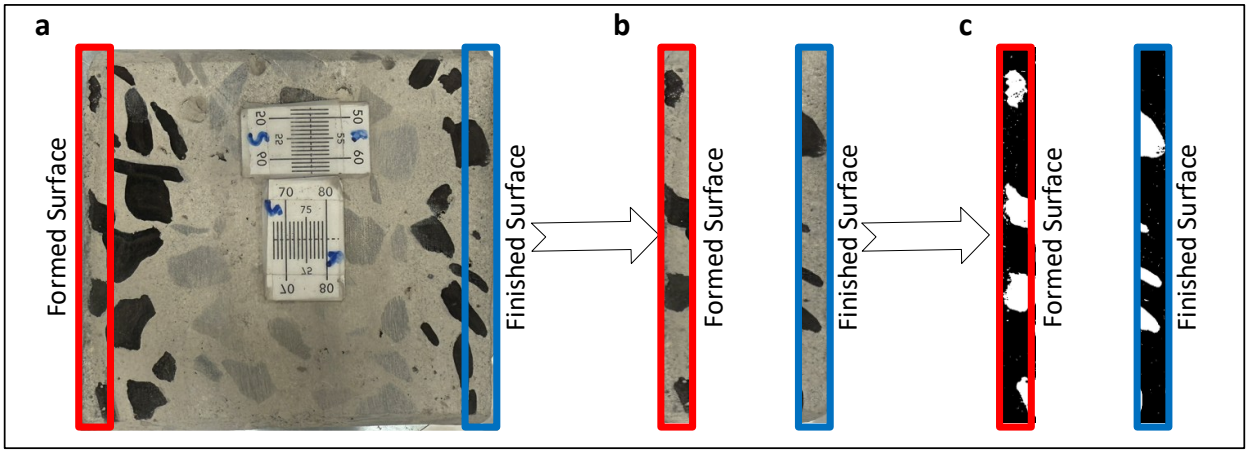

Fig. 2—Example of: (a) a painted concrete section, (b) cropped 5-mm slices from finished and formed surfaces, and (c) binary images from ImageJ.

2.7 Nitrogen Sorption

To quantify mortar quality at the surface, five small pieces of mortar were extracted from each of the finished and formed surfaces (top 5 mm) of concrete cores taken from OPC5 and PLC5 slab samples. The extracted samples were then oven-dried at 105 °C for 24 hours before testing by Nitrogen sorption. The samples were then transferred to different sample tubes and dried for an additional 3 hours at 60 ± 2 °C in a nitrogen-rich environment. Micromeritics Tristar II Plus instrument was implemented to investigate the pore structure characteristics under a pressure of 100 kPa of liquid nitrogen. The Barrett-Joyner-Halenda (BJH) method was utilized to examine the distribution of pore size and pore volumes of the samples [55, 56]. Additionally, the nitrogen sorption method was used to measure the surface area of raw PLC and OPC samples. 100 mg of anhydrous cement powder samples from different sources were oven-dried at 60 ± 2 °C for approximately 24 hours. Then, the samples were placed in separate sample tubes and further dried at 60 ± 2 °C for 3 hours in a nitrogen-rich environment. The surface area of the anhydrous cement samples was investigated using the Brunauer-Emmett-Teller (BET) method [57].

2.8 Accelerated Carbonation Testing

Early-age carbonation of concrete could cause early delamination of concrete floors. Therefore, the carbonation rate of PLC and OPC systems is determined using an accelerated carbonation testing procedure. After 28 days of curing, 50 mm slices were cut from the cylinders for carbonation. Then, the samples were oven-dried at 60 °C to attain a 70% degree of saturation (DOS). Prepared concrete samples were carbonated in a carbonation chamber at 23 ± 1 °C and a relative humidity of 70% for 60 days. A constant low-pressure CO_2 flow (≈1 psi) with a concentration of 4 ± 0.1% was used in the carbonation chamber.

To measure the depth of carbonation, after the carbonation period, each slice was split into two parts and then sprayed with a 1% phenolphthalein indicator on the fractured surface. The fractured surface of concrete turns to a red-purple color for a pH of 9.5 or higher (not a carbonated region) and becomes colorless at lower pH values (carbonated region). After the phenolphthalein application, the depth of

carbonation was measured using a caliper at several locations with higher, lower, and medium levels of carbonation, and the average value was reported.

2.9 Results and Discussion

2.9.1 Effects of Physical/Chemical Characteristics of Cement on Fresh and Hardened Concrete

The relationship between the BET surface area (m^2/g) and the required HRWR to achieve target slump for different concrete mixtures (w/c=0.42) with various cement types is illustrated in Fig. 3, which indicates that HRWR demand generally increases with an increase in BET surface area. This trend can be attributed to the fact that a higher BET surface area implies a greater amount of fine particles within the cement, which increases the overall surface area requiring wetting [20, 58]. As the surface area increases, a higher dosage of HRWR is needed to disperse these particles effectively and achieve the desired workability. OPC samples (OPC1, OPC4, OPC5) have a lower BET surface area compared to PLC samples. BET surface areas for OPC samples range approximately between 1.0–1.1 m^2/g, while PLC samples span a wider range, approximately from 1.3–1.9 m^2/g. The increased HRWR requirement for PLCs is, therefore, a direct consequence of their physical characteristics, particularly their higher specific surface area due to the inclusion of finely ground limestone, as shown in Fig. 3. Fig. 4 indicates that the BET surface area tends to increase as the calcite content increases.

Among the OPC mixtures, the OPC5 mixture required a substantially higher HRWR dosage, even when compared to other OPCs with similar BET surface areas. The increased HRWR requirement for OPC5 can partially be explained by its higher C_3S content (Table 2). Higher C_3S content can increase the early hydration rate and, consequently, the HRWR demand to attain the required workability.

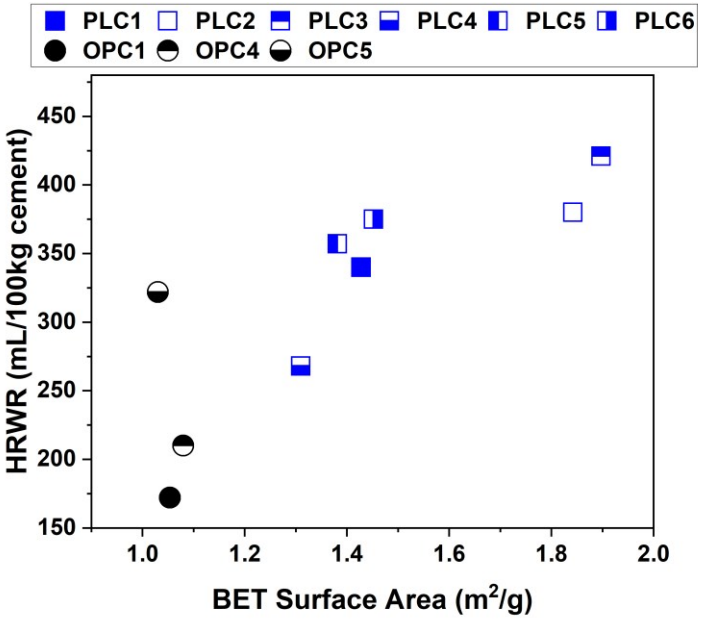

Fig. 3—Required HRWR dosage as a function of measured surface area for OPC and PLC samples (w/c=0.42).

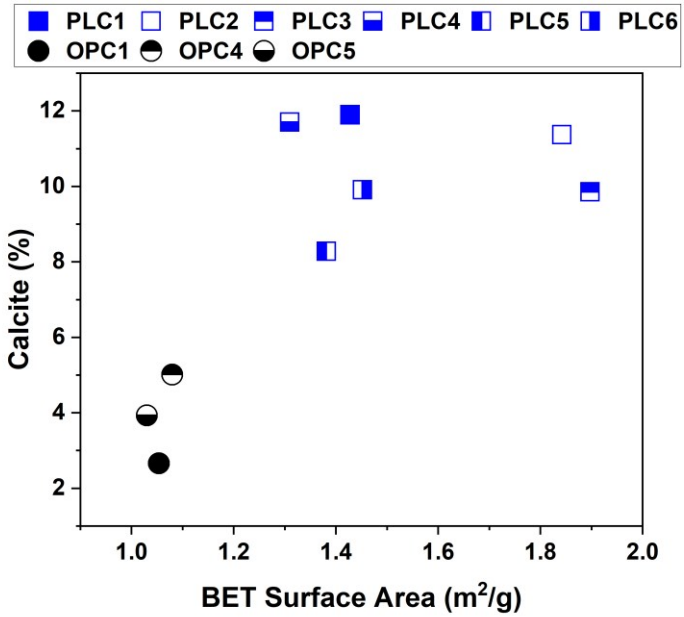

Fig. 4—Effect of calcite content on measured surface area of OPC and PLC samples.

Fig. 5 illustrates the compressive strength of OPC and PLC mixtures with varying w/c after 28 days of curing. Overall, PLC mixtures exhibited comparable or slightly greater compressive strength when compared to OPC mixtures from the same source (except the mixtures with a w/c of 0.42 from source 4). The average compressive strength among different sources of PLC is about 6-10% higher than that of OPC sources (Fig. 5). This is partially attributed to the filler effect of limestone particles (Fig. 6), which refines the microstructure. The finer limestone particles (<5 μm) effectively fill the interstitial voids between the larger cement grains (10-30 μm), increasing the packing density of the paste and reducing the capillary porosity. Fig. 6 indicates that the compressive strength of PLC samples considerably increases as the BET surface area (i.e., fineness of particles) increases. Based on Fig. 6, PLC from source 4 has the lowest fineness among different PLCs, which can explain the lower compressive strength values obtained for the PLC4-0.42 mixture. In addition, limestone particles can serve as nucleation sites to enhance hydration and microstructure development [11, 19]. Further, Fig. 7 demonstrates that the combined content of C_3S and C_2S has an impact on the compressive strength of PLC and OPC samples. This is expected since C_3S and C_2S are the primary clinker phases that contribute to the formation of calcium silicate hydrate (C-S-H), which is largely responsible for the strength development in cementitious systems [59, 60]. This superior performance of PLCs can be attributed to synergistic effects, such as enhanced particle packing, filler effects, and potentially better hydration characteristics due to limestone interactions [11, 16, 18].

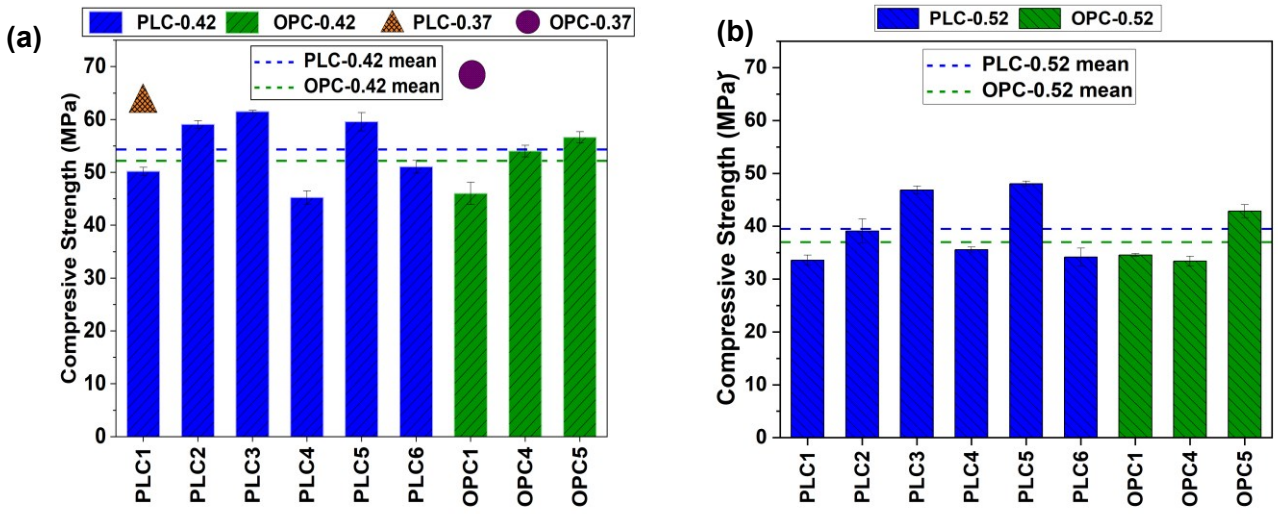

Fig. 5—Compressive strength of OPC and PLC samples as a function of w/c after 28 days of curing: (a) w/c = 0.37 & 0.42, and (b) w/c= 0.52.

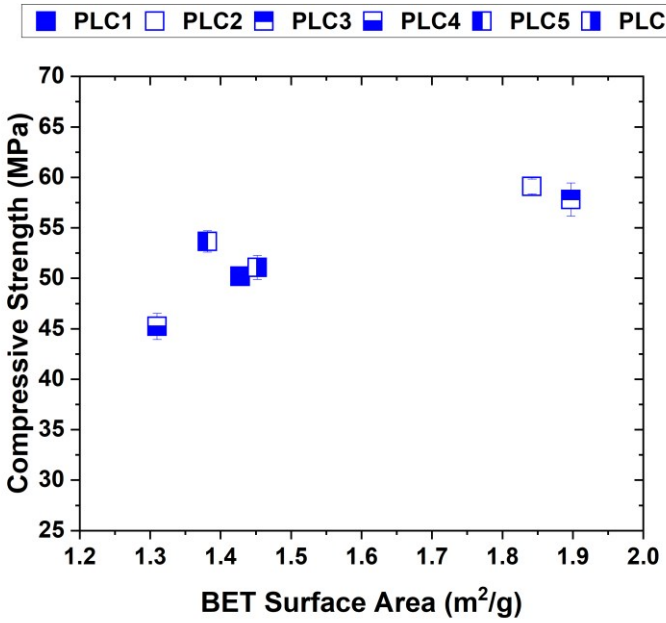

Fig. 6—Impact of BET surface area on compressive strength of PLC mixtures with w/c of 0.42.

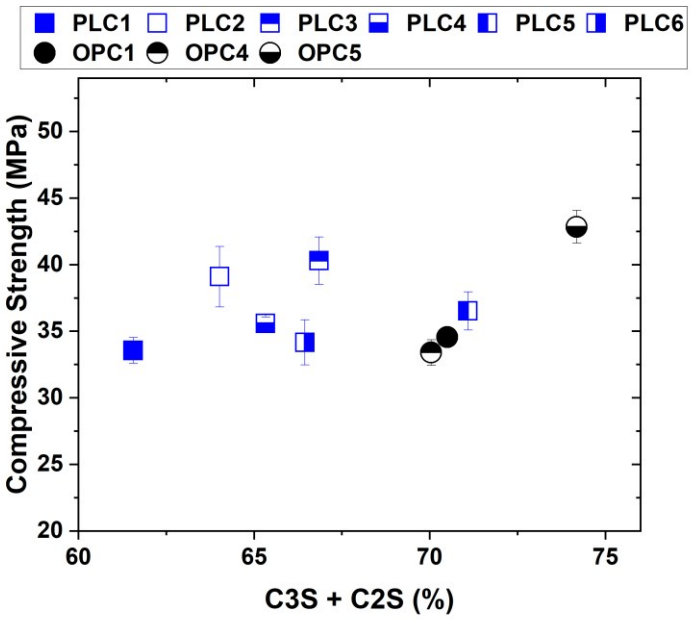

Fig. 7—Impact of "C_3S+C_2S" content on compressive strength of PLC and OPC mixtures with w/c of 0.52.

The scatter plot in Fig. 8 presents the relationship between HRWR dosage and compressive strength for concrete mixtures with a w/c of 0.42, including both PLC and OPC. The results indicate that an increase in HRWR dosage generally leads to an improvement in compressive strength for both PLC and OPC mixtures. The increase in compressive strength as a function of HRWR dosage can be attributed to HRWR's ability to enhance the dispersion of cement particles due to the steric hindrance provided by the Polycarboxylate Ether (PCE) HRWR admixture, leading to improved hydration and reduced porosity in the hardened matrix. It seems that the effect of HRWR dosage on the compressive strength of PLC mixtures is more apparent due to the finer particle size of PLCs. This can be attributed to the higher HRWR dosages required for high-fineness PLCs, which result in superior deflocculation of the cement and limestone particles. Overall, a combination of physical and chemical characteristics of PLC impacts the fresh and hardened properties of concrete. Therefore, these characteristics of PLC need to be optimized in order to balance its enhanced sustainability with performance in concrete applications.

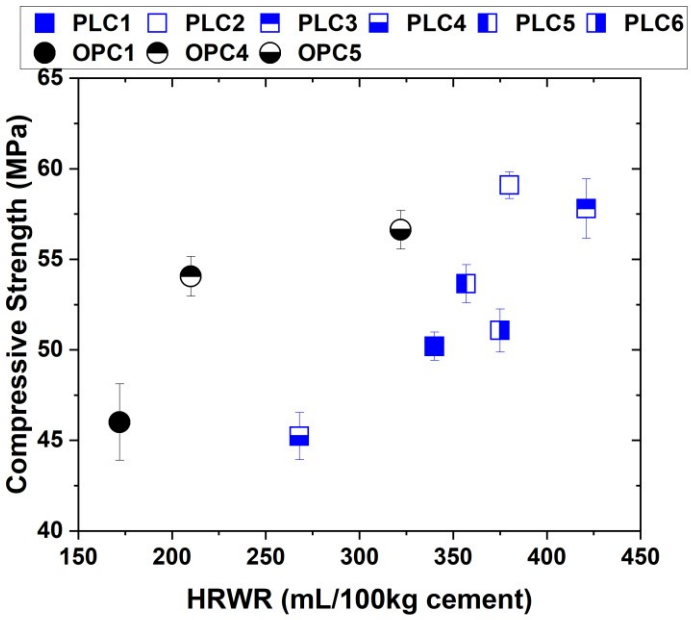

Fig. 8—Effect of HRWR dosage on compressive strength of PLC and OPC mixtures with w/c of 0.42.

2.9.2 Abrasion Resistance

The results of the accelerated abrasion resistance test (AART) are shown in Fig. 9 (using a box and whisker plot with 25th, 50th, and 75th percentiles) for the OPC and PLC mixtures with varying w/c for both finished and formed surfaces. Fig. 9 also includes the normal distribution of measured average abrasion depth values from different mixtures (3 replicates per mixture). Additionally, Fig. 10 presents the abrasion depth as a function of compressive strength for finished and formed surfaces.

At w/c of 0.52, on average, PLC systems demonstrated better performance on finished surfaces compared to OPC systems. OPC samples had an average wear depth of 3.41 mm, whereas PLC had an average wear depth of 2.69 mm. However, the variability of abrasion depth (between sources) in PLC samples (1.5-4.0 mm) is higher than in OPC samples (2.8-4.0 mm). This can be attributed to the variation in physical (e.g., fineness) and chemical properties (e.g., C_3S content) of PLC samples, as discussed earlier. For instance, a PLC system with a higher fineness can lead to improved particle packing and better abrasion resistance, especially in high w/c mixtures. Based on Dhir et al. [24], the addition of 15% ground limestone showed a minimal impact on the abrasion resistance of concrete. But, with increasing limestone content (>15%), the abrasion depth was found to become gradually higher than that of OPC concrete [24]. At w/c of 0.42, PLC mixtures showed a comparable abrasion performance to OPC mixtures on finished surfaces. Based on results from finished surfaces, the abrasion depth of OPC/PLC mixtures with a w/c of 0.42 is approximately 40-50% lower than that of the OPC/PLC mixtures with a w/c of 0.52. At a w/c ratio of 0.37, both OPC and PLC mixtures achieved the best abrasion resistance. This improvement in abrasion resistance with a decrease in w/c can be explained by the increase in compressive strength results, as shown in Fig. 10. Fig. 10a indicates that there is a linear negative relationship between abrasion depth (of finished surfaces) and compressive strength of the mixtures, irrespective of the cement type. This is because the abrasion resistance of concrete is greatly influenced by the microstructure of the surface

matrix. A reduction of w/c near the surface of the concrete can improve the matrix compaction and compressive strength of the system. These observations are in accordance with findings from previous studies on OPC and OPC+SCM mixtures [31]. Overall, Fig. 10a shows that PLC mixtures are as resistant to abrasion as OPC mixtures when compared at relatively equal strengths. This supports the viability of PLC as a low-clinker alternative to OPC in high-wear applications.

Based on Fig. 9, the formed (bottom) surface shows considerably lower abrasion depth compared to the finished (top) surface for both OPC and PLC systems. On average, a 25-55% reduction in abrasion depth of the formed surfaces was observed compared to that of the finished surfaces. This behavior can be explained by the difference in concentration of coarse aggregates in finished and formed surfaces, as well as the quality of the paste matrix (i.e., local porosity and degree of densification) at the surface. These phenomena have been further discussed in the next sections. As discussed, the obtained data on the formed surface (with no bleeding phenomenon and denser paste matrix) can represent a concrete floor with a good quality surface finish. Overall, the impact of cement type and w/c on the abrasion depth of formed surfaces is limited, except for PLC samples with a w/c of 0.52, which displayed a slightly higher abrasion depth compared to other mixtures.

At a w/c ratio of 0.37, OPC samples show a minimal abrasion value of 0.38 mm, while PLC samples demonstrate a remarkably low abrasion value of 0.18 mm. As discussed, lower w/c results in denser microstructure and reduced porosity, enhancing the concrete's ability to resist wear. Based on Fig. 10b, the abrasion depth in formed surfaces is linearly decreased as a function of compressive strength. For the samples with a higher compressive strength (> 60 MPa), the abrasion depth is negligible in the formed surfaces. Furthermore, a surface hardener applied on PLC1 0.52 samples demonstrated a substantial enhancement in abrasion resistance. The finished surface with surface hardener exhibited an average abrasion depth of 0.45 mm, whereas the formed surface with surface hardener displayed an average abrasion depth of 0.04 mm. These measurements correspond to reductions in abrasion depth of approximately 80% and 90%, respectively, when compared to PLC1 0.52 without surface hardener. However, their effective service life and the need for reapplication in industrial settings should be examined.

As discussed, based on BS 8204-2: 2003 [47], the allowable maximum depth of wear for light-duty industrial floors (compressive strength of ≈40 MPa) is 0.4 mm. Based on the results of this study, the abrasion depths measured on the finished surface of the OPC and PLC samples are considerably higher than this limit, except for the sample with surface hardener. However, the measured abrasion depths on formed surfaces of OPC and PLC samples with a higher compressive strength (> 50 MPa) are comparable to the specified limit. This observation emphasizes that the abrasion resistance of concrete greatly depends on compressive strength (i.e., microstructure quality) and surface finishing condition (i.e., paste thickness and quality). Further research is required to examine the performance of the developed mixtures in industrial settings in order to provide reliable performance-based criteria.

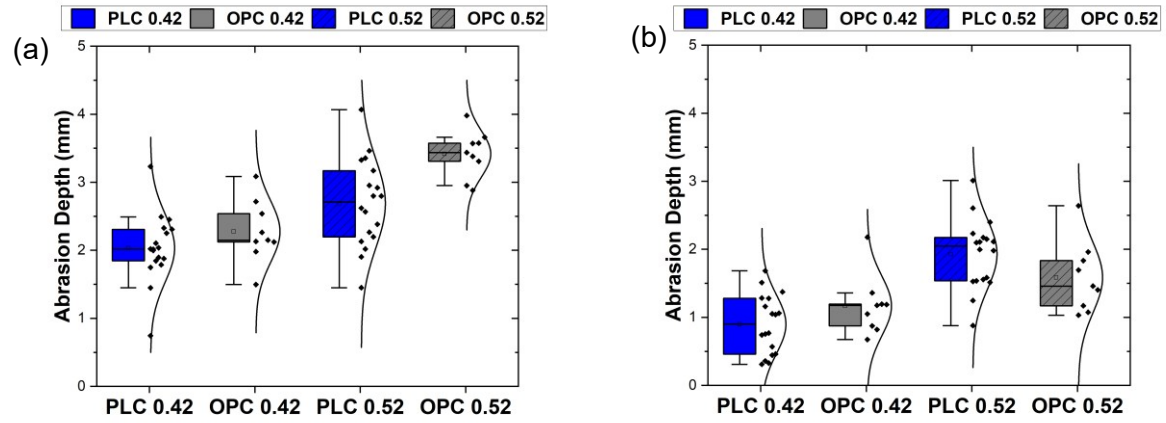

Fig. 9—Abrasion depth for OPC and PLC slabs with varying w/c: a) finished surface and b) formed surface.

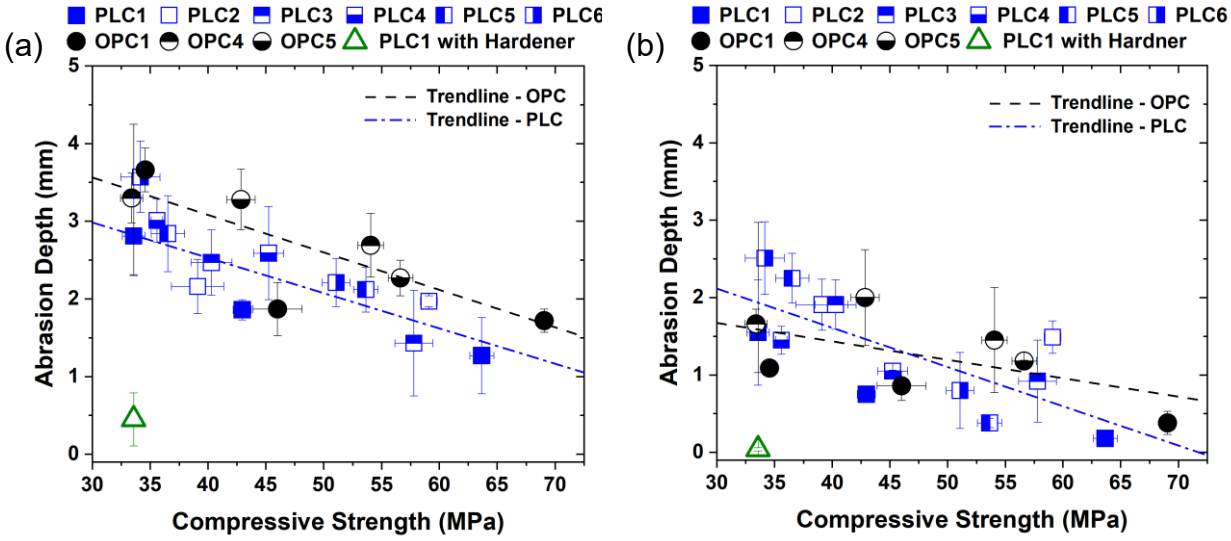

Fig. 10—Abrasion depth of OPC and PLC mixtures as a function of compressive strength: a) finished surface and b) formed surface.

2.9.3 Mortar Content at Finished/Formed Surfaces

Fig. 11 demonstrates the examples of OPC and PLC concrete sections with calculated mortar content based on cropped 5-mm slices from finished and formed surfaces. Additionally, the box plot, shown in Fig. 12, provides a comparative analysis of mortar content (% of the area) in different concrete surfaces at the analyzed top 5 mm sections using binary images. The data indicate that finished surfaces have, on average, 10-15% higher mortar content compared to formed surfaces, irrespective of the cement type. This is because finishing processes typically lead to an increase in mortar content through the migration of fine particles to the surface, while reducing the exposure of coarse aggregates. Additionally, during vibration, denser aggregates settle toward the formed face, while lower-density fine particles migrate to

the finished surface. As a result, the finished surface is more paste-rich. This means that the abrasion resistance of finished surfaces is largely impacted by the quality of paste and fine aggregates. Formed surfaces, in contrast, exhibit lower mortar content, likely due to their uniform compaction. Hence, the abrasion resistance of formed surfaces is partially dependent on the quality of exposed coarse aggregate. As illustrated in Fig. 13, the abrasion resistance of the tested concrete samples diminishes as the mortar content at the surface increases, irrespective of cement type and w/c. These findings partly explain the difference between the abrasion resistance of finished and formed surfaces. Previous studies also discussed the importance of surface conditioning and finishing methods to attain abrasion-resistant surfaces [34, 61-62].

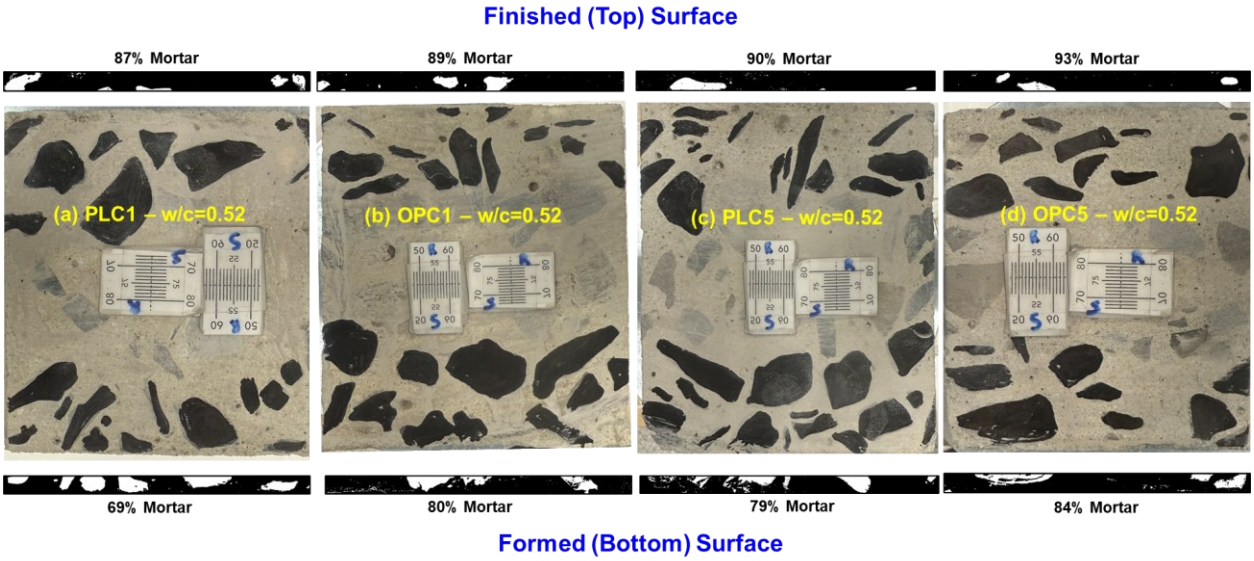

Fig. 11—Examples of OPC/PLC concrete sections with calculated mortar content based on cropped 5-mm slices from finished and formed surfaces: (a) PLC1-w/c=0.52, (b) OPC1-w/c=0.52, (c) PLC5-w/c=0.52, and (d) OPC5-w/c=0.52.

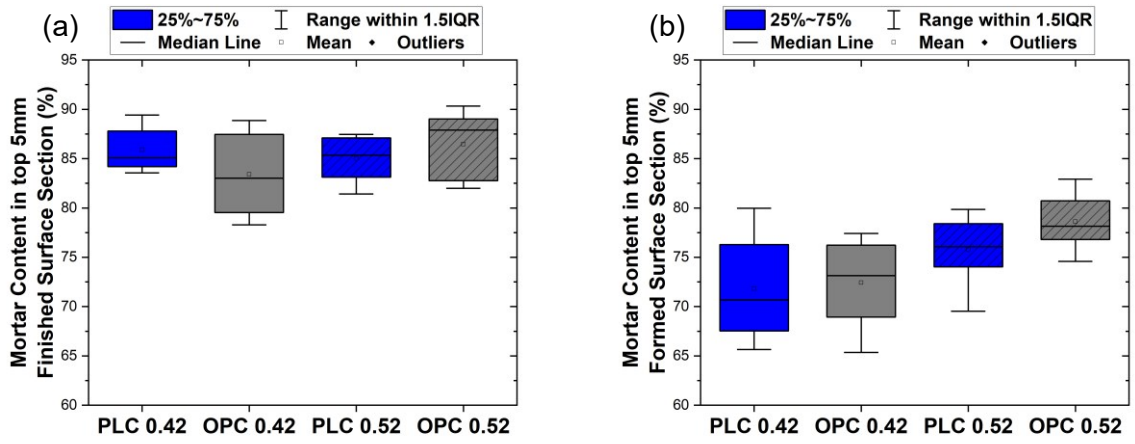

Fig. 12—Mortar Content of PLC and OPC concrete mixtures in top 5 mm: a) finished surface and b) formed surface.

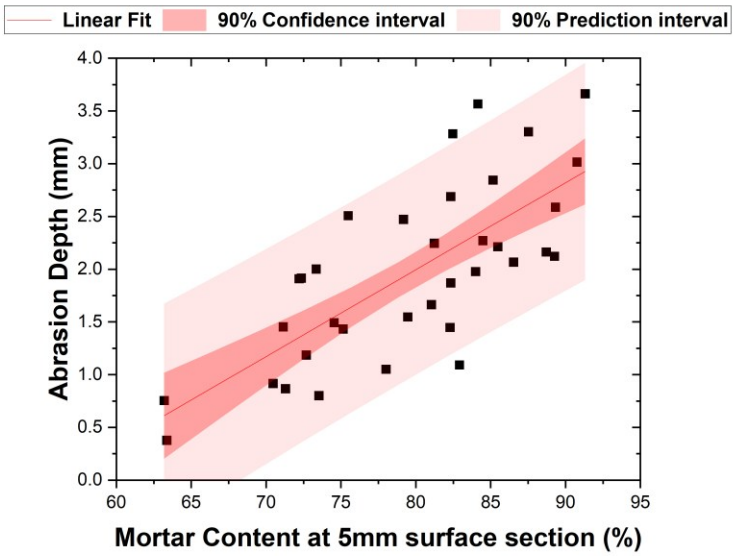

Fig. 13—Relationship between abrasion depth and mortar content at the surface of concrete samples with varying w/c and cement type.

2.9.4 Pore Size Distribution in Finished/Formed Surfaces

Pore size distribution curves obtained from the nitrogen sorption experiment for OPC5 and PLC5 samples (mortar portion) with a w/c of 0.52 for finished and formed surfaces are shown in Fig. 14. There is a clear difference in the volume of micropores in the range of 3-20 nm for finished and formed surfaces, regardless of the cement type. It appears that the porosity of the paste matrix for the finished surface is higher due to the bleeding/fresh settlement effect. This can result in lower abrasion resistance for finished surfaces compared to formed surfaces. Previous research demonstrated that hand finishing is less effective in eliminating capillary channels from the concrete surface when compared to power finishing methods [34, 63].

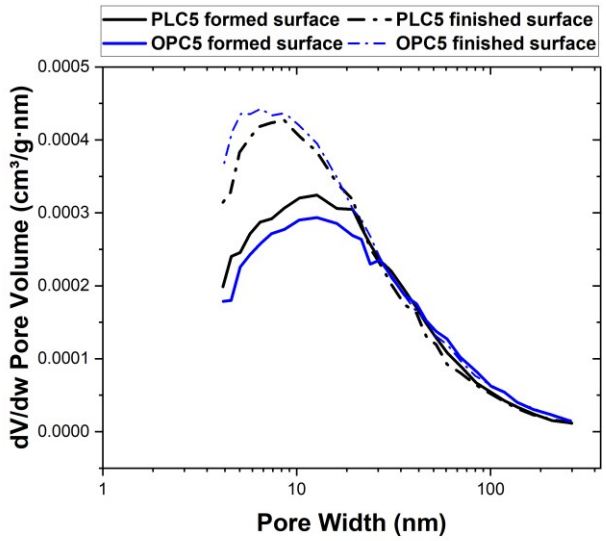

Fig. 14—Pore Size distribution for finished and formed surfaces of PLC5 and OPC5 samples (mortar portion) with a w/c of 0.52.

2.9.5 Carbonation Depth

Fig. 15 shows the measured average carbonation depth for different OPC and PLC systems as a function of w/c. Based on Fig. 15, PLC and OPC samples show a similar performance, and there is no statistically significant difference between the carbonation depth of OPC and PLC samples. As expected, the carbonation depth is greater in higher w/c OPC and PLC systems. A 70% increase in the carbonation depth of 0.52 w/c samples was observed when compared to the 0.42 w/c samples.

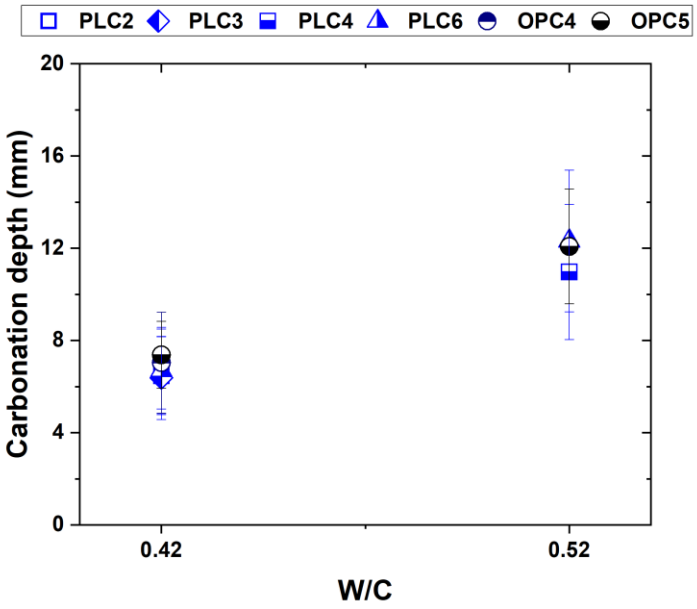

Fig. 15—Carbonation depth of OPC and PLC mixtures as a function of w/c.

2.9.6 Practical Considerations and Limitations

It is important to contextualize these laboratory findings within the constraints of industrial construction. The abrasion resistance results presented in this study correspond to concrete mixtures designed to achieve nominal compressive strength levels of approximately 40 MPa, 50 MPa, and 60 MPa through variation in the w/c. Comparative evaluation of PLC and OPC concrete was therefore conducted across these strength levels under controlled mixture conditions. A single source of coarse aggregate (dolomitic limestone) and fine aggregate (river sand) was used throughout the experimental program in this phase to determine the effects of cement type, cement source, and w/c on abrasion resistance. This also helped to study a reasonable number of PLC and OPC sources from different regions of the US to demonstrate the variation in the performance. While the materials used are representative of standard structural concrete, high-wear industrial floors may utilize harder aggregates (e.g., granite, trap rock) or dry-shake hardeners or fibers to meet stricter classifications. Furthermore, the manual finishing techniques employed in this study generate lower surface shear forces than the ride-on power trowels used in large-scale slab construction. Consequently, the absolute abrasion depths reported here may be different compared to those of field-consolidated slabs. However, the relative performance trends between PLC and OPC remain valid, as both systems were subjected to similar consolidation, curing, and finishing regimes.

Additionally, the abrasion resistance of both finished (top) and formed (bottom) surfaces was measured to quantify the impact of surface finishing conditions on the abrasion depth. While the formed surface is not exposed to abrasion in industrial floors, the obtained data on the formed surface (with no bleeding phenomenon and denser paste matrix) can represent a concrete floor with a good-quality surface finish.

2.10 Conclusions

This phase investigated the abrasion resistance of portland limestone cement (PLC) systems with varying w/c from six different sources/producers and the comparison with those of ordinary portland cement (OPC) systems according to BS EN 13892-4:2003. Additionally, the influence of the test surface (finished surface versus formed surface) and the impact of a surface hardener on the abrasion resistance of PLC and OPC mixtures were evaluated. The following conclusions can be drawn:

- The abrasion resistance of PLC concrete was found to be comparable to or greater than that of OPC concrete when evaluated at similar compressive strength levels, indicating that PLC can meet performance requirements for high-wear industrial floor applications.
- Higher variability in abrasion resistance among PLC sources (compared to OPC sources) was observed, which is attributed to differences in the physical and chemical characteristics of the PLCs, including cement fineness and clinker–limestone composition.
- Increased cement fineness in PLC systems enhanced compressive strength through improved particle packing (filler effect), but also resulted in higher high-range water-reducing (HRWR) admixture demand to achieve target workability. Appropriate HRWR dosages improved cement and limestone particle dispersion and hydration efficiency, contributing to strength development.
- The abrasion resistance of concrete improved with decreasing water-to-cement ratio (w/c) for both OPC and PLC mixtures. At lower w/c ratios (0.37), both cement types showed significantly better abrasion resistance, directly linked to improved compressive strength and denser microstructural formation at the concrete surface.

- The abrasion depth was negatively correlated with compressive strength, with minimal abrasion observed in surfaces with strengths exceeding 60 MPa.
- Formed (bottom) surfaces exhibited consistently higher abrasion resistance compared to finished (top) surfaces, attributed primarily to lower mortar content (i.e., more uniform distribution of coarse aggregates at the formed surface) and the quality of the paste.
- The finished surfaces showed, on average, 10-15% higher mortar content compared to formed surfaces, irrespective of the cement type. Additionally, pore size distribution analyses revealed higher porosity at finished (top) surfaces due to bleeding effects, contributing to reduced abrasion resistance.
- The application of surface hardener notably enhanced abrasion resistance. Treated PLC concrete surfaces demonstrated reductions in abrasion depth by approximately 80-90% compared to untreated PLC surfaces, highlighting the significant potential of surface treatments in improving durability for high-wear concrete applications.
- The measured abrasion depths on formed surfaces of OPC and PLC samples with a higher compressive strength (> 50 MPa) are comparable to the specified limit by BS 8204-2: 2003 for light-duty industrial floors. This observation emphasizes that the abrasion resistance of concrete greatly depends on compressive strength (i.e., microstructure quality) and surface finishing condition (i.e., paste thickness and quality).
- PLC and OPC samples show a similar carbonation performance, and there is no statistically significant difference between the carbonation depth of OPC and PLC samples.

Overall, the results emphasize that abrasion resistance is governed by a combination of compressive strength, cement characteristics, water-to-cement ratio, and surface condition.

3 Abrasion Resistance of Portland Limestone Cement Concrete Incorporating Supplementary Cementitious Materials and Fiber Reinforcement

Phase 1 established that properly wet-cured PLC concrete can achieve abrasion resistance comparable to, or better than, OPC concrete at similar w/c ratios. However, industrial floor mixtures rarely consist of plain cement systems. In practice, supplementary cementitious materials (SCMs) are widely used to reduce clinker content and embodied carbon. Additionally, fiber reinforcement is commonly added to control plastic and drying shrinkage cracking. Further, alternative surface treatment strategies, such as lithium silicate sealer (i.e., a penetrating densifier), are employed to densify the surface matrix and accommodate construction schedules. The combined influence of these variables on the abrasion resistance of PLC concrete remains insufficiently quantified.

Building upon the baseline performance established in phase 1, this section investigates the abrasion resistance of PLC concrete incorporating slag, fly ash, fiber reinforcement, and lithium silicate densifier. The same testing methodology, curing comparison framework, and surface characterization techniques used in section 2 are applied to ensure direct comparability and continuity between phases.

3.1 Materials

The PLC and OPC used in Phase 2 were the same materials used in Phase 1. This ensured consistency in clinker composition, limestone content, and fineness. The PLC control mixture and OPC control mixture in this phase correspond directly to the Phase 1 PLC1 and OPC1 mixtures at a w/c of 0.52, enabling direct comparison between phases. Ground granulated blast furnace slag (GGBFS) conforming to ASTM C989 with a specific gravity of 2.84 and Class F fly ash (FA) conforming to ASTM C 618-25 with a specific gravity of 2.36 were used as partial cement replacements (20-50%). Based on X-ray fluorescence analysis (Table 4), the slag contains approximately 43% CaO and 33% SiO_2, indicating a calcium-rich SCM with latent hydraulic properties. The fly ash contained approximately 54% SiO_2 and 26% Al_2O_3, with low CaO content, characteristic of a low calcium pozzolan.

Table 4—Chemical Composition of GGBFS and FA from XRF.

Chemical Composition (%)	SCMs	
	Slag1	**FA1**
SiO_2	32.60	54.06
Al_2O_3	14.37	26.42
Fe_2O_3	0.42	8.08
CaO	43.38	2.6
MgO	5.73	1.72
K_2O	0.38	2.86
Na_2O	0.18	0
SO_3	1.11	0
LOI	1.00	2.45

A macro-synthetic polypropylene fiber designed for industrial floor applications was incorporated in selected PLC mixtures at a dosage of approximately 2.97 kg/m³. The fibers are 54 mm long, non-corrosive, and designed to enhance crack control. They are inert and do not chemically interact with the cement matrix. The fibers were uniformly dispersed during mixing and were intended to provide crack control and surface integrity.

The same coarse and fine aggregates described in section 2 were used for all Phase 2 mixtures. Aggregate gradation and mineralogy were held constant to isolate the effects of binder composition, fibers, and surface densifier. A polycarboxylate-based high-range water-reducing (HRWR) admixture was used as required to maintain workability at a constant w/b of 0.52. The HRWR dosage varied by mixture, reflecting differences in binder type. The slag and fly ash mixtures required moderate dosages, while the fiber-reinforced mixtures required substantially higher dosages. Additionally, a lithium silicate-based sealer/densifier with a specific gravity of 1.10 (with <20% lithium silicate content) was utilized to evaluate its efficacy in improving the abrasion resistance of PLC systems.

3.2 Mixture Proportioning

All Phase 2 mixtures were proportioned at a single w/b of 0.52. This value was deliberately selected based on both practical relevance. Industrial floor concrete is commonly placed at w/b between approximately 0.50 and 0.55 to achieve adequate workability, finishing response, and constructability for large slab-on-ground placements. Additionally, results from Phase 1 demonstrated that abrasion resistance differences between PLC and OPC systems were clearly distinguishable at a w/b of 0.52, whereas lower w/b exhibited reduced sensitivity to mixture modifications due to an inherently denser paste structure. The total binder content was kept constant at approximately 342 kg/m³ in all mixtures. Table 5 summarizes the mixture proportions. FA and GGBFS were used in concrete mixtures to replace 20-50% of the weight of the PLC. Varying dosages of HRWR based on the type of cementitious materials and fiber addition were used to maintain the target workability of 100 mm. The slag and fly ash mixtures required moderate dosages, while the fiber-reinforced mixtures required substantially higher dosages. The mixtures included:

OPC1: 100% OPC from source 1, for reference. This is identical to the Phase 1 OPC1-0.52 mixture.

PLC1: 100% PLC from source 1. This is identical to the Phase 1 PLC1-0.52 mixture.

PLC1+Slag1-50%: 50% GGBFS + 50% PLC1.

PLC1+Slag1-25%: 25% GGBFS + 75% PLC1.

PLC1+FA1-20%: 20% Class F fly ash + 80% PLC.

PLC1+Fiber: 100% PLC1 + fibers (2.97 kg/m³).

PLC1+Densifier: 100% PLC1, with lithium-silicate densifier/sealer.

PLC1+Fiber+Densifier: 100% PLC + fibers (2.97 kg/m³), with lithium-silicate densifier/sealer.

Table 5—Mixture design of concrete mixtures (Phase 2) in a saturated surface dry (SSD) condition.

Mixture	OPC1	PLC1	PLC1+Slag1-25%	PLC1+Slag1-50%	PLC1+FA1-20%	PLC1+Fiber
Coarse Aggregate	990	990	988	990	987	986
Fine Aggregate	854	854	851	854	849	850
Cement	342	342	257	168	274	342
Fly Ash	0	0	0	0	68	0
Slag	0	0	86	168	0	0
Fibers	0	0	0	0	0	2.97
Water	178	178	178	175	178	178
HRWR (g/100 kg cement)	0	0	250	324	270	565

3.3 Sample Preparation and Curing

A similar mixing procedure as Phase 1 was used, except for the mixtures with fiber. In fiber mixtures, fibers were added to coarse and fine aggregates in dry form and mixed for two minutes to achieve initial homogeneity and avoid agglomeration of the fibers. Subsequently, cement and water, with pre-dissolved HRWR, were added to the mixture. The complete mixture was then thoroughly mixed for an additional five minutes to ensure optimal dispersion of the cementitious materials, fiber, and admixture throughout the aggregate matrix.

Similar to Phase 1, rectangular prism-shaped concrete slabs measuring 525 × 512.5 × 100 mm^3 were prepared for abrasion testing. Cylindrical samples (100 mm × 200 mm) were also prepared for compressive strength measurements. The samples were sealed for the first 24 hours using polyethylene sheeting to limit moisture loss during early hydration. After demolding, the samples were wet cured for 14 days at 23 °C by covering both finished and formed surfaces with burlap maintained in a continuously saturated (dripping) condition. After wet curing, the samples underwent 13 days of dry air curing at a controlled temperature of 23 ± 2 °C to simulate typical drying conditions encountered by industrial floor systems. All the samples were tested at 28 days.

For samples with a lithium silicate densifier, the surface densifier was sprayed on top after the completion of the finishing process and when the final set is achieved. A microfiber applicator was then used to uniformly spread the densifier to thoroughly coat the concrete surface. According to the manufacturer's instructions, the concrete surface was kept wet for 15-20 minutes. Then, the samples were wet cured for 14 days at 23 °C, followed by 13 days of dry air curing.

The experimental methods followed those detailed in section 2.

3.4 Results and Discussion

3.4.1 Compressive Strength

Fig. 16 illustrates the compressive strength of Phase 2 mixtures after 28 days of curing. The mixture with 25% slag exhibited comparable compressive strength to PLC and OPC mixtures, while the mixture with 50% slag showed a 13% lower strength. This is because the hydration in slag materials is slower due to

their lower reactivity [64, 65]. Slag exhibits a slower initial dissolution compared to OPC/PLC [66]. This is mainly attributed to the lower Ca/Si ratio in GGBFS. Additionally, there is an approximately 25% reduction in compressive strength when 20% of the PLC was replaced with Class F FA. This is attributed to the lower pozzolanic reactivity of Class F FAs due to lower calcium content. The addition of the macro fibers slightly improved the compressive strength.

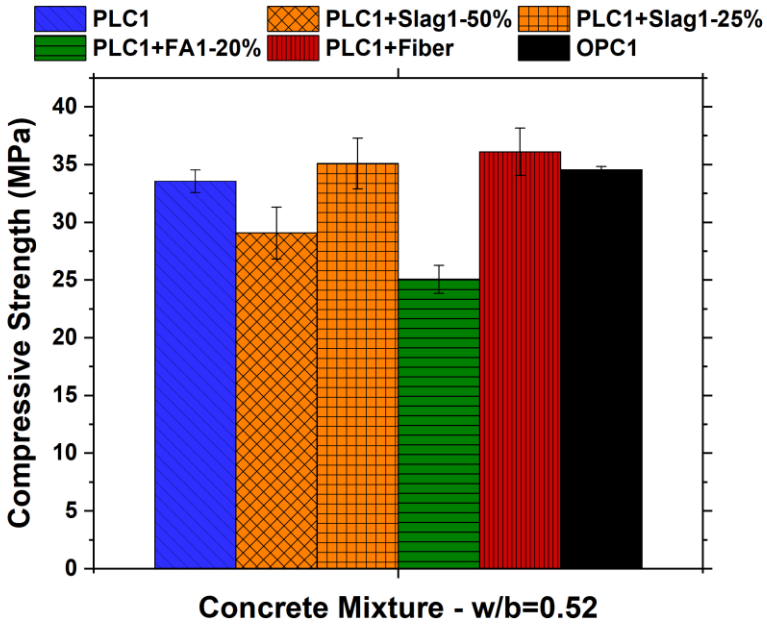

Fig. 16—Compressive strength of PLC+SCM and PLC+Fiber samples versus control OPC and PLC mixtures after 28 days of curing (w/b=0.52).

3.4.2 Abrasion Resistance

Fig. 17 shows the abrasion resistance of PLC+SCM mixtures versus control OPC and PLC mixtures as a function of compressive strength for finished and formed surfaces. Additionally, Fig. 18 illustrates the impact of macro fibers, surface densifier, and their combination on the abrasion depth for the finished surface. On average, a 17-21% increase in abrasion depth of the finished surfaces of PLC+FA and PLC+Slag samples was observed when compared to control PLC samples. A similar trend was seen for the formed surfaces of PLC+FA and PLC+Slag samples. This can be partially explained by the lower compressive strength of PLC+SCM samples at 28 days compared to control OPC and PLC samples. This is attributed to the slow hydration/pozzolanic reaction in slag and FA systems. As discussed in section 2, the higher abrasion depth of finished surfaces compared to formed surfaces is linked to higher mortar fractions and higher porosity of the matrix in finished surfaces than in formed surfaces.

Based on Fig. 18, the addition of macro fibers reduced the abrasion depth of PLC systems by 15-25%. This can be attributed to the enhanced toughness of fiber-reinforced concrete due to the interlocking network of fibers that hold the matrix together. However, there is no impact from the application of a lithium silicate-based surface densifier.

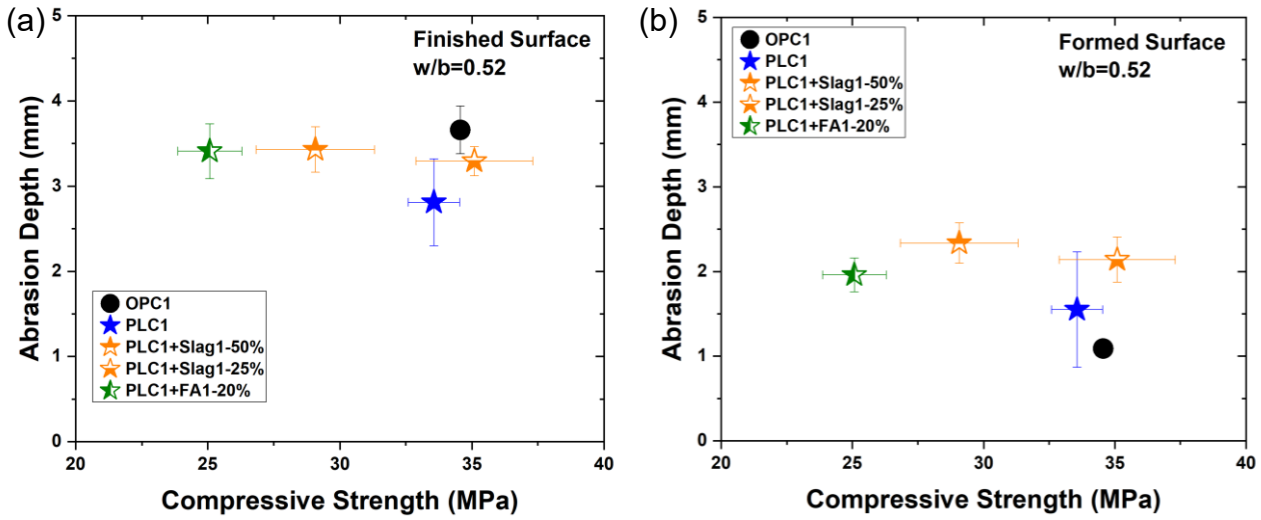

Fig. 17—Abrasion depth of PLC+SCM mixtures versus control OPC and PLC mixtures as a function of compressive strength: a) finished surface and b) formed surface.

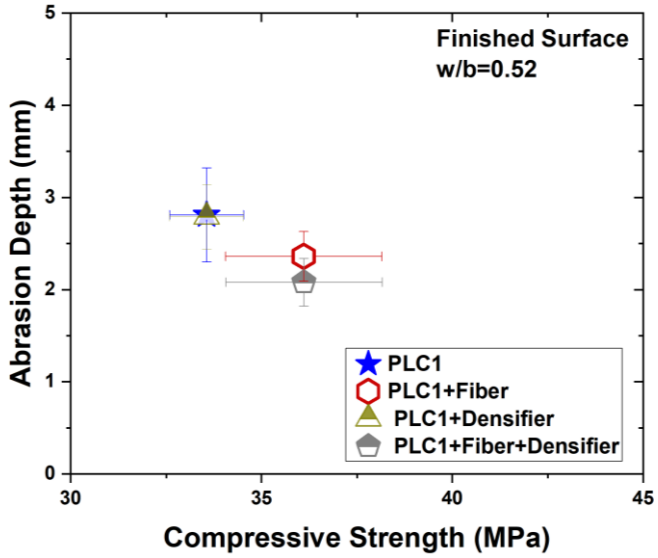

Fig. 18—Impact of macro fibers, surface densifier, and their combination on the abrasion depth.

3.5 Conclusions

This phase of the study investigates the abrasion resistance of PLC concrete in combination with SCMs (slag and fly ash), macro-synthetic fiber reinforcement, and lithium-silicate densifier/sealer. All mixtures were tested at a w/b ratio of 0.52 for 28-day abrasion and compressive strength. The following conclusions can be drawn:

- PLC with 50% slag showed 22% higher abrasion with a 13% lower strength, while 25% slag reduced the increase to 17%.
- PLC with 20% Class F fly ash increased finished surface abrasion by 21% and reduced strength by 25%.
- Fiber reinforcement with synthetic macro fibers reduced abrasion depth by up to 25 percent relative to control PLC samples.
- Lithium silicate densifier illustrated no effect on the abrasion resistance of PLC systems.

4 Abrasion performance of PLC and PLC+SCM systems in the field

Abrasion measurements in industrial settings are necessary to establish a correlation between lab measurements and field performance, and to develop performance-based specifications. Temple University, in collaboration with Concrete Strategies LLC, designed and tested several concrete slabs with PLC in combination with different SCMs in St. Louis, Missouri (Fig. 19). A 5.5 × 5.5 m² slab with a thickness of 20 cm was cast for each mixture. All mixtures contained fibers (4.45 kg/m^3). A lithium silicate-based surface densifier/sealer was used as a curing compound. These field concrete mixtures were also replicated and tested in the Concrete Materials Laboratory at Temple University using the same constituent materials collected from the field. Additionally, paste mixtures were prepared to examine the impact of lithium silicate-based curing compound on microstructure versus sealed curing.

Fig. 19—Accelerated Abrasion Resistance Testing in the field, St. Louis, Missouri.

4.1 Materials

Type IL cement (identified as PLC7), complying with ASTM C595, sourced from Missouri, was used. Ground granulated blast furnace slag conforming to ASTM C989 (identified as Slag2) and Class C fly ash conforming to ASTM C 618-25 (identified as FA2) were used as partial cement replacements (20-25%). The chemical composition of PLC7, Slag2, and FA2 samples, as identified by X-ray fluorescence (XRF), is listed in Table 6. Based on XRD analysis, PLC7 contains 8.31% calcite and 1.24% dolomite.

The coarse aggregate used was a crushed high-quality limestone with a nominal maximum aggregate size of 19 mm. The coarse aggregate possesses a specific gravity of 2.68 and an absorption capacity of 1.1%. For the fine aggregate, siliceous natural river sand was used with a specific gravity of 2.63 and an absorption rate of 0.30%. To ensure the workability of the concrete mixture while maintaining the w/c, a combination of polycarboxylate-based high-range water reducer (HRWR) and mid-range water reducer (MRWR) was incorporated. The HRWR+MRWR was used to achieve and sustain a target slump of 100 ± 12.5 mm, in compliance with common workability requirements for industrial floor systems. Additionally, a lithium silicate-based sealer/densifier with a specific gravity of 1.10 (with <20% lithium silicate content) was utilized as a curing compound.

A macro-synthetic polypropylene fiber designed for industrial floor applications was incorporated in all mixtures at a dosage of approximately 4.45 kg/m³. The fibers are 54 mm long, non-corrosive, and designed to enhance crack control. They are inert and do not chemically interact with the cement matrix. The fibers were uniformly dispersed during mixing and were intended to provide crack control and surface integrity.

Table 6—Chemical composition of PLC7 and SCMs from XRF.

Chemical Composition (%)	Cement Type and Source		
	PLC7	Slag2	FA2
SiO_2	19.09	32.78	36.64
Al_2O_3	4.52	10.47	20.00
Fe_2O_3	3.06	1.14	5.35
CaO	62.58	42.27	19.61
MgO	2.12	11.00	5.35
K_2O	0.59	0.45	0.87
Na_2O	0.10	0.23	6.01
SO_3	3.08	0.77	2.39
LOI	4.51	0.03	1.07

4.2 Mixture Proportioning and Placement and Testing

Three concrete mixtures were prepared. These mixtures were delivered by the ready-mix supplier for casting slabs in the field. All Phase 3 mixtures were proportioned at a single w/b of 0.48. Mixture 1 was a control PLC mixture with no SCM. Mixture 2 used FA2 to replace 20% of the weight of the PLC. Mixture 3 was prepared with 25% Slag2. Table 7 summarizes the mixture proportions. As discussed, a macro-synthetic polypropylene fiber designed for industrial floor applications was incorporated in all mixtures at a dosage of approximately 4.45 kg/m³.

Field slabs: A 5.5×5.5 m^2 slab with a thickness of 20 cm was cast for each mixture in the parking lot (Fig. 19). After placement, the concrete surface was first struck off and then lightly floated to level the surface. Final finishing was performed after the bleed water had dissipated and the surface had reached a suitable stiffness. Power-troweling equipment (8' rider) was utilized for finishing the slabs. When the final set was achieved, the lithium silicate-based surface densifier was sprayed on top. A microfiber applicator was then used to uniformly spread the densifier to thoroughly coat the concrete surface. According to the manufacturer's instructions, the concrete surface was kept wet for 15-20 minutes. Then, the slabs were air-dry-cured for 28 days (May 17 – June 15). The average daily temperature and relative humidity (RH) and total precipitation during the curing period of slabs are presented in Fig. 20.

Lab slabs: For lab testing, rectangular prism-shaped concrete slabs measuring 525 × 512.5 × 100 mm^3 were prepared for abrasion testing. After placement, the concrete surface was first struck off using a straightedge and then lightly floated to level the surface. Final finishing was performed after the bleed water had dissipated and the surface had reached a suitable stiffness. Two consistent passes were applied using a steel hand trowel under uniform pressure to achieve a smooth and consistent surface texture.

Then, the lithium silicate-based surface densifier was sprayed on top after the completion of the finishing process and when the final set is achieved. A microfiber applicator was then used to uniformly spread the densifier to thoroughly coat the concrete surface. According to the manufacturer's instructions, the concrete surface was kept wet for 15-20 minutes. Then, the samples were cured at room temperature for 28 days.

After 28 days, the accelerated abrasion resistance test (AART) was performed following BS EN 13892-4:2003 at four different locations per slab in the field (Fig. 19). For the lab investigation, three replicate slab samples (finished surfaces) were tested per mixture. Additionally, cylindrical samples (100 mm × 200 mm) were prepared for compressive strength measurements. The compressive strength samples were wet cured inside saturated limewater for 28 days at 23 °C.

Table 7—Mixture design of concrete mixtures (Phase 3) in a saturated surface dry (SSD) condition.

Mixture	PLC7	PLC7+Slag2-25%	PLC7+FA2-20%
Coarse Aggregate	1035	1025	1023
Fine Aggregate	834	839	837
Cement	344	258	275
Fly Ash	0	0	69
Slag	0	86	0
Fibers	4.45	4.45	4.45
Water	165.5	165.5	165.5

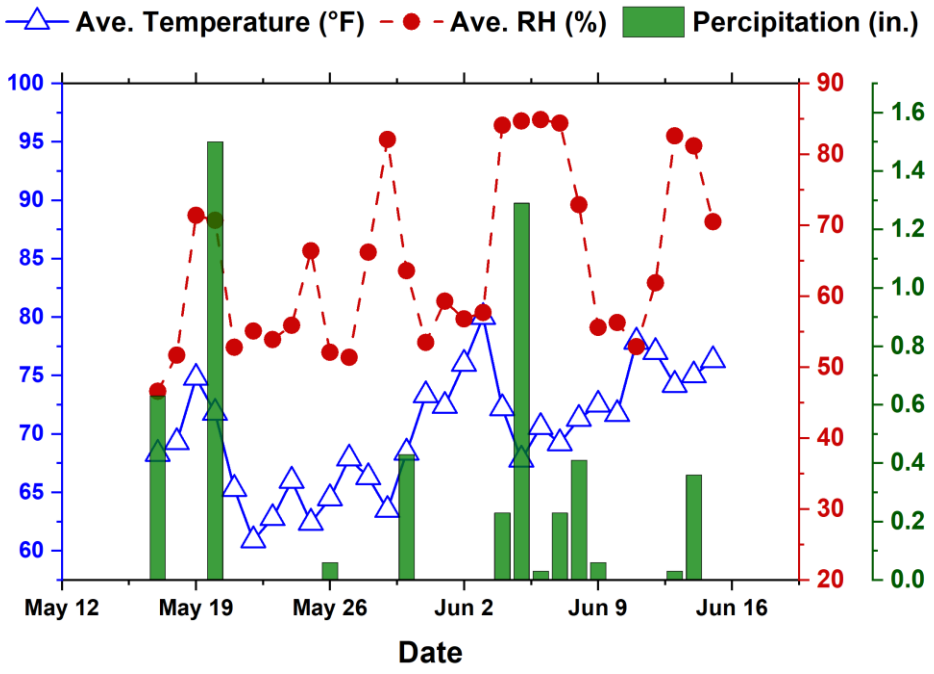

Fig. 20—Average daily temperature and relative humidity (RH) and precipitation during the curing period of slabs, St. Louis, Missouri (data are taken from https://www.wunderground.com/).

Paste mixtures: Three paste mixtures were prepared to quantify the impact of the lithium silicate-based curing compound on microstructure. For the paste mixtures, the proportions from Table 7 (excluding the aggregates and fibers) were utilized. Cylindrical paste samples (50 × 102 mm) were cast. The samples were cured using two different curing methods: sealed curing for 28 days at 23 °C, and using a lithium silicate-based curing compound. For the lithium silicate-based curing compound, similar application and curing procedures to those of concrete slabs were used.

After curing, samples for thermogravimetric analysis (TGA) were taken from the top surface (first 5 mm) and inner portion (i.e., middle) of the paste sample. These samples were ground to a fine powder in a laboratory ball mill and sieved through a #200 sieve to obtain a homogeneous powder with particles smaller than 75 μm. The samples were dried using a solvent-exchange method. About 5 grams of the powdered sample were taken after sieving, mixed with 50 mL of isopropyl alcohol (IPA), and left to rest for 15 minutes. IPA helps stop ongoing hydration reactions and replaces pore water in the sample. After equilibration, the suspension was filtered through a Büchner funnel under vacuum for 5 minutes. To further remove residual IPA and aid drying, the filter cake was rinsed with 10 mL of diethyl ether. During this step, the vacuum pump was temporarily turned off to allow gentle interaction between the solvent and the sample. The vacuum was then reapplied for an additional 5 minutes or until the sample appeared visibly dry. The dried residue was carefully collected, sealed in airtight plastic bags, and stored in closed containers to prevent rehydration and carbonation before TGA analysis.

For the TGA procedure, approximately 40 mg of the dried sample was placed in a 100 μL platinum crucible. Testing involved allowing the sample to equilibrate for 15 minutes at 25 °C under a continuous stream of nitrogen gas to reach a stable mass. The temperature was then ramped to 40 °C and held for 5 minutes. Next, the sample was heated from 40 °C to 950 °C at a rate of 20 °C/min to complete the test. This process ensured the identification of all reaction phases in the system.

4.3 Results and Discussion

4.3.1 Abrasion Resistance

Fig. 21 compares the abrasion depth of PLC+SCM mixtures and the control PLC mixture as a function of compressive strength from field and lab testing. Overall, the field testing showed a very limited abrasion depth (0.03-0.11 mm) compared to lab measurements (2.5-4.0 mm). Based on our observation, the difference in quality of surface finishing (power fishing versus hand finishing) creates this discrepancy between field and lab measurements. Previous research by Sadegzadeh et al. [34] reported that the finishing technique utilized heavily impacts the abrasion resistance of concrete. According to their experiments, repeated power finishing yielded the best results by compacting the paste matrix and eliminating capillary channels at the surface. Overall, the lab measurements (from Phase 3) are slightly higher than those from Phase 1 (the trendline from Phase 1 measurements is shown in Fig. 21b). This can be partially attributed to the difference in curing methods utilized (wet curing versus lithium silicate-based curing compound). This has been extensively discussed in the following, using TGA measurements.

Based on Fig. 21, the mixture with 20% Class C FA and 25% slag showed a comparable or better performance when compared to the control PLC samples, except for the 25% slag mixture from the field. The mixture with 25% slag has the highest abrasion depth among the field samples, while its compressive strength is the highest. It should be noted that the compressive strength samples were wet cured; however, the slabs were air-cured after application of lithium silicate curing compound. This can be partially

attributed to the temperature and relative humidity fluctuations during the curing in the field (Fig. 20). Application of proper curing method and duration is critical in slag-based systems due to their lower reactivity (i.e., slower hydration). Enhanced abrasion performance of the fly ash system can be because of the higher reactivity of Class C ash, considering high calcium oxide content, and also very high alkali content.

Nevertheless, based on BS 8204-2: 2003, all field slabs with PLC and PLC+SCM satisfy the allowable maximum depth of wear for medium-duty industrial floors (abrasion depth < 0.2 mm). Considering the correlation between lab and field data, it seems that most of the PLC mixtures from Phase 1 can provide satisfactory abrasion resistance for medium-duty industrial floors by utilizing an enhanced surface finishing procedure.

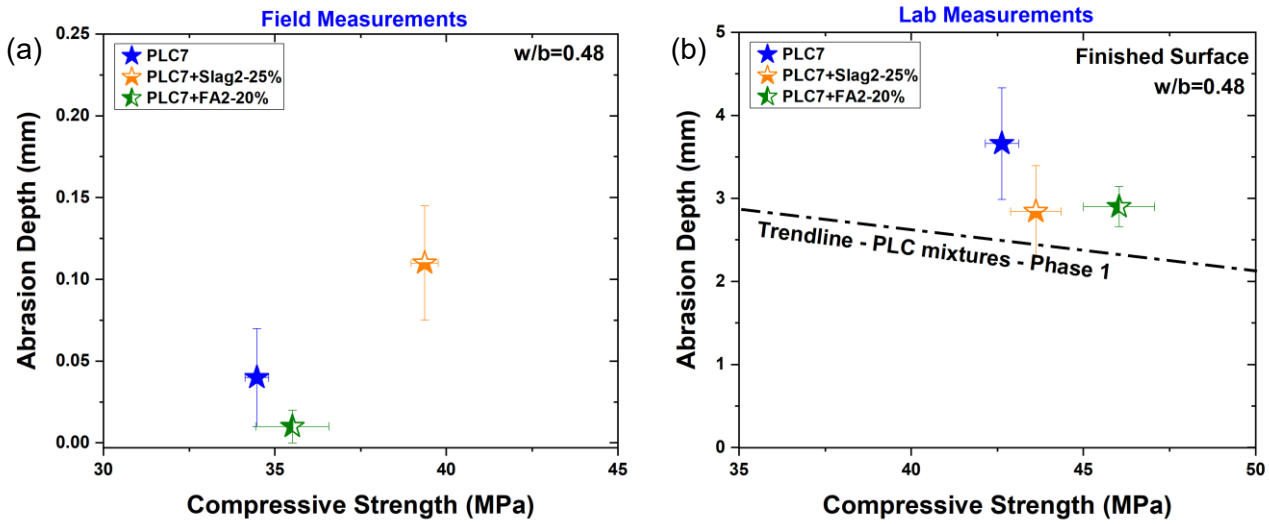

Fig. 21—Abrasion depth as a function of compressive strength for PLC and PLC+SCM mixtures: (a) field measurements and (b) lab results.

4.3.2 Impact of Curing Method on Surface Microstructure

As discussed, paste mixtures were prepared to examine the impact of lithium silicate-based curing compound on microstructure compared to sealed cured samples. Fig. 22 depicts TGA weight loss and derivative thermogravimetry (DTG) profiles of three different paste mixtures. Fig. 22 compares the microstructure of the top surface for sealed cured and lithium silicate cured samples. It is noticeable that there is a considerable difference in the TGA profiles between sealed cured and lithium silicate cured samples for all mixtures. Sealed cured samples showed higher weight loss due to decomposition of C-S-H/AFt (50-200 °C) and $Ca(OH)_2$ (400-500 °C) compared to lithium silicate cured samples. However, the lithium silicate cured samples present higher weight loss due to decomposition of carbonates (500-800 °C). These results demonstrate that the degree of hydration is lower in the top surface (first 5 mm) of lithium silicate cured samples. This can be attributed to the lower effectiveness of the lithium silicate curing compound in sealing the capillary pores to avoid or minimize pore water evaporation. These observations suggest that eliminating the wet curing can lead to poor microstructure at the surface of

concrete slabs, and consequently can adversely affect abrasion performance, especially in SCM systems with low reactivity.

Fig. 23 illustrates the calculated hydration and carbonation products and chemically bound water from TGA for different paste mixtures. It compares the measurements at the top surface to those at the inner portion (i.e., middle) of the lithium silicate cured samples. Based on Fig. 23, while the amount of hydration products at the surface of lithium silicate cured samples is substantially lower (30-50%) than that of sealed cured ones, the inner portion of the lithium silicate cured samples has a comparable amount of hydration products to the sealed cured samples. As discussed, this difference in the surface microstructure of lithium silicate cured samples can lead to inadequate abrasion resistance for industrial floors. A comparison of abrasion results from Phase 1 (wet cured, Fig. 10a), Phase 2 (lithium silicate cured + wet cured, Fig. 18), and Phase 3 (lithium silicate cured, Fig. 21b) supports this finding.

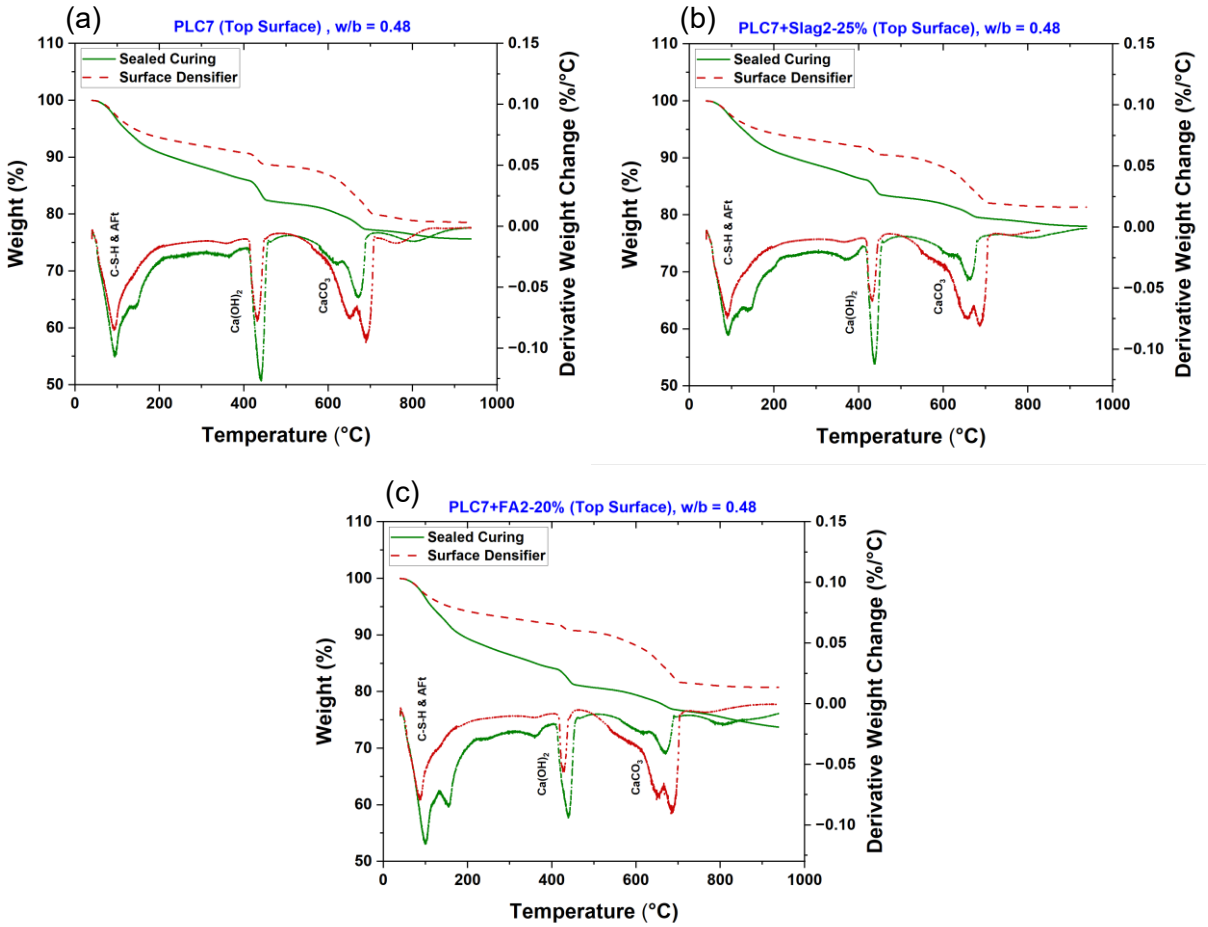

Fig. 22—TGA weight loss and DTG profiles of paste samples (top surface) with sealed curing versus lithium silicate-based curing compound: (a) PLC7, (b) PLC7+Slag2-25%, and (c) PLC7+FA2-20%.

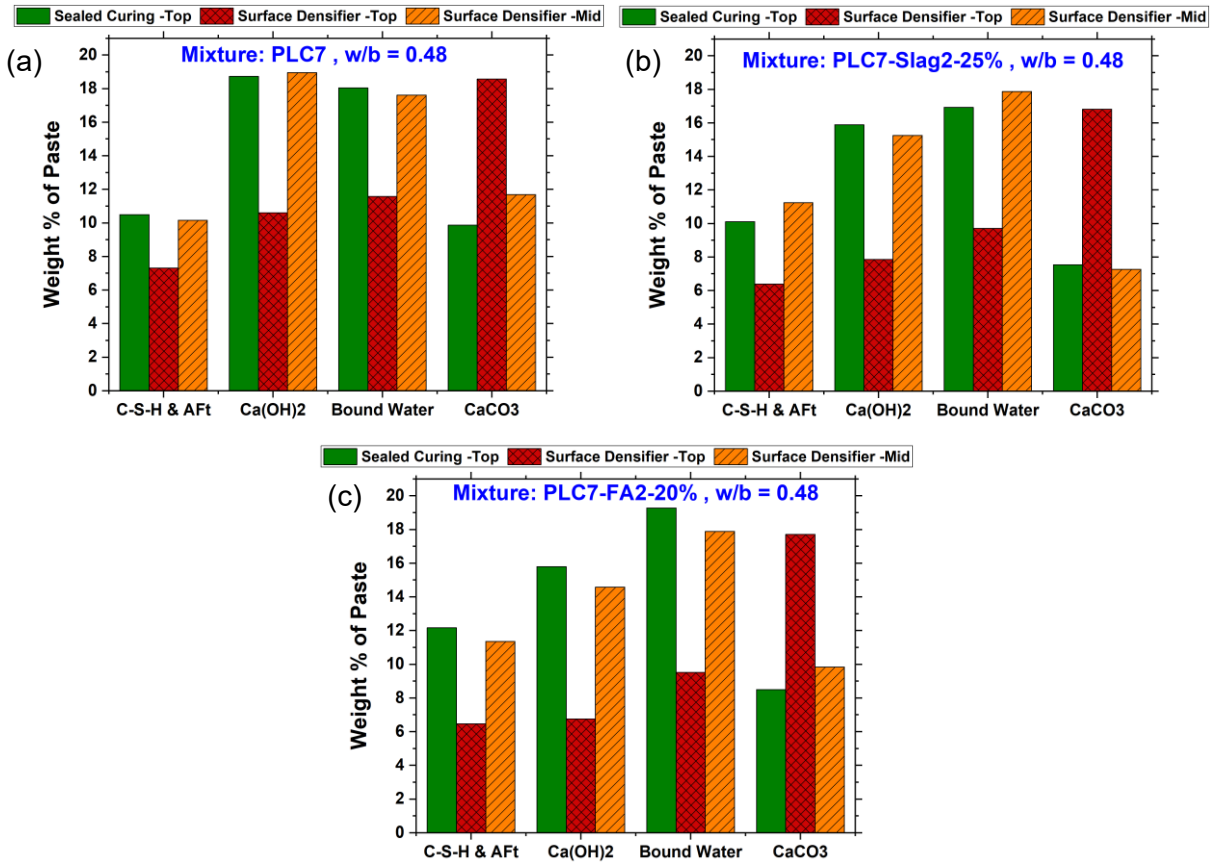

Fig. 23— Calculated hydration and carbonation products of paste samples (top surface (Top) vs. inner portion of the sample (Mid)) with sealed curing versus lithium silicate-based curing compound: (a) PLC7, (b) PLC7+Slag2-25%, and (c) PLC7+FA2-20%.

4.4 Conclusions

This phase of the study established a correlation between abrasion measurements in the lab and field settings. Three concrete mixtures with PLC in combination with slag and Class C fly ash were examined. All mixtures contained macro synthetic fibers. A lithium silicate-based surface densifier/sealer was used as a curing compound. Additionally, paste mixtures were prepared to examine the impact of lithium silicate-based curing compound on microstructure compared to sealed curing. The following conclusions can be drawn:

- Field samples showed a very limited abrasion depth (0.03-0.11 mm) compared to the lab samples (2.5-4.0 mm). This is mainly attributed to the difference in quality of surface finishing (power fishing versus hand finishing) between field and lab measurements.
- Overall, PLC+SCM mixtures showed a comparable or better performance when compared to the control PLC samples.
- All field slabs with PLC and PLC+SCM satisfy the allowable maximum depth of wear for medium-duty industrial floors (abrasion depth < 0.2 mm) according to BS 8204-2: 2003.

- Lithium silicate cured paste samples demonstrate a lower degree of hydration (a 30-50% lower amount of hydration products) at the surface (first 5 mm) compared to sealed cured samples. This can lead to porous microstructure at the surface of lithium silicate-cured samples, consequently inadequate abrasion resistance for industrial floors.

5 References

1. “North America Concrete Flooring Market Size, Share & Trend Analysis Report By Product (Coated, Polished), By Application (Residential, Commercial), By Region, And Segment Forecasts, 2023 - 2030", Report ID: GVR-4-68040-059-6, Grand View Research, 2023. https://www.grandviewresearch.com/industry-analysis/north-america-concrete-flooring-market-report# (last accessed: 5/4/2025),

2. Garber, G. “ Design and construction of concrete floors”, *CRC Press*, 2nd Edition, 2019.

3. CR Concrete, "Amazon Project Rose," https://crconcrete.pro/amazon-project-rose-2/ (last accessed: 5/4/2025),

4. Bribián, I. Z., Capilla, A. V., and Usón, A. A., "Life cycle assessment of building materials: Comparative analysis of energy and environmental impacts and evaluation of the eco-efficiency improvement potential," *Building and Environment*, V. 46, No. 5, 2011, pp. 1133-40.

5. ASTM C150/C150M – 24, "Standard Specification for Portland Cement," ASTM International, West Conshohocken, PA, 2024, 9 pp.

6. ASTM C595/C595M − 24, "Standard Specification for Blended Hydraulic Cements," ASTM International, West Conshohocken, PA, 2024, 9 pp.

7. Tennis, P., Thomas, M., and Weiss, W., "State-of-the-Art Report on Use of Limestone in Cements at Levels of up to 15%," PCA R&D SN3148, *Portland Cement Association*, Skokie, IL. 2011.

8. Hooton, R.D. and Riding, K.A., 2025. "Type IL cement use in precast, prestressed concrete," *PCI Journal*, V. 70, No. 2, 2025, pp. 23-36. https://doi.org/10.15554/pcij70.2-04.

9. Schmidt, M., Middendorf, B., and Singh, N. B., "Blended Cements" Chapter 10 in *Modern Cement Chemistry*. 2010.

10. ACI Committee 302, 2015, "Guide to Concrete Floor and Slab Construction (ACI PRC-302.1-15)," American Concrete Institute, Farmington Hills, MI, 76 pp.

11. Barrett, T. J., Sun, H., Nantung, T., and Weiss, W. J., "Performance of Portland limestone cements," *Transportation Research Record*, V. 2441, No. 1, 2014, pp. 112-20. https://doi.org/10.3141/244

12. Thomas, M. D., Hooton, D., Cail, K., Smith, B. A., De Wal, J., and Kazanis, K. G., "Field trials of concretes produced with portland limestone cement," *Concrete International*, V. 32, No. 1, 2010, pp. 35-41.

13. Meddah, M. S., Lmbachiya, M. C., and Dhir, R. K., "Potential use of binary and composite limestone cements in concrete production," *Construction and Building Materials*, V. 58, 2014, pp. 193-205. https://doi.org/10.1016/j.conbuildmat.2013.12.012

14. Bucher, B. E., "Shrinkage and shrinkage cracking behavior of cement systems containing ground limestone, fly ash, and lightweight synthetic particles." *Purdue University ProQuest Dissertations & Theses*, 2009, 1476093.

15. Barrett, T., Sun, H., Villani, C., Barcelo, L., and Weiss, J., "Early-Age Shrinkage Behavior of Portland Limestone Cement," *Concrete International*, V. 36, No. 2, 2014.

16. Alexander, M. G., "Durability performance potential and strength of blended Portland limestone cement concrete," *Cement and Concrete Composites*, V. 39, 2013, pp. 115-21. https://doi.org/10.1016/j.cemconcomp.2013.03.027

17. Thomas, M. D., and Hooton, R. D., "The durability of concrete produced with portland-limestone cement: Canadian studies," PCA R&D SN3142, *Portland Cement Association*, Skokie, IL, V. 5, No. 28, 2010, 6 pp.

18. Berke, N. S., Inceefe, A. N., Kramer, A., and Antommattei, O. R., "Durability of Portland Limestone Cement Concrete," *Concrete International*, V. 44, No. 1. 2022, pp. 34-9.

19. Bazarbekova, A., Shon, C-S., Kissambinova, A., Zhang, D., and Kim, J., "Evaluating the Efficacy of Limestone Powder as a Partial Replacement of Ordinary Portland Cement for the Sustainable Stabilization of Sulfate-Bearing Saline Soil," *Sustainability*, V. 16, No. 21, 2024, pp. 9224. https://doi.org/10.3390/su16219224

20. Hansen, B. S., Howard, I. L., Shannon, J., Cost, T., and Wilson, W. M., "Portland-limestone cement fineness effects on concrete properties," *ACI Materials Journal*, V. 117, No. 2, 2020, pp. 157-68. https://doi.org/10.14359/51720301

21. Cost, V. T., Howard, I. L., and Shannon, J., "Improving concrete sustainability and performance with use of Portland–limestone cement synergies," *Transportation Research Record*, V. 2342, No. 1, 2013, pp. 26-34. https://doi.org/10.3141/2342-

22. Bharadwaj, K., Chopperla, K.S.T., Choudhary, A., Glosser, D., Ghantous, R.M., Vasedevan, G., Ideker, J.H., Isgor, B., Trejo, D., and Weiss, W.J., "CALTRANS: impact of the use of Portland-limestone cement on concrete performance as plain or reinforced material-final report," Corvallis, OR: Oregon State University. https://doi.org/10.5399/osu/1150.

23. Sharma, A., Sirotiak, T., Wang, X., Taylor, P., and Angadi, P., "Portland Limestone Cement for Reduced Shrinkage and Enhanced Durability of Concrete," *Magazine of Concrete Research,* Vol. 73 No. 3, 2021, pp. 147–162. https://doi .org/10.1680/jmacr.19.00165.

24. Dhir, R., Limbachiya, M., McCarthy, M., and Chaipanich, A., "Evaluation of Portland limestone cements for use in concrete construction," *Materials and Structures*, V. 40, 2007, pp. 459-73. https://doi.org/10.1617/s11527-006-9143-7

25. Scott, B. D., and Safiuddin, M., "Abrasion Resistance of Concrete--Design, Construction and Case Study," *Concrete Research Letters*, V. 6, No. 3, 2015.

26. Li, H., Zhang, M., and Ou, J., "Abrasion resistance of concrete containing nano-particles for pavement," *Wear*, V. 260, No. 11-12, 2006, pp. 1262-6. https://doi.org/10.1016/j.wear.2005.08.006

27. Warudkar, A., and Elavenil, S., "A comprehensive review on abrasion resistance of concrete," *International Journal of Applied Science and Engineering*, V. 17, No. 1, 2020, pp. 29-43. 10.6703/IJASE.202003_17(1).029

28. Laplante, P., Aitcin, P-C., and Vezina, D., "Abrasion resistance of concrete," *Journal of Materials in Civil Engineering*, V. 3, No. 1, 1991, pp. 19-28. https://doi.org/10.1061/(ASCE)0899-1561(1991)3:1(19

29. Dhir, R., Hewlett, P., and Chan, Y., "Near-surface characteristics of concrete: abrasion resistance," *Materials and Structures*, V. 24, 1991, pp. 122-8. https://doi.org/10.1007/BF02472473

30. Atis C. D., "High volume fly ash abrasion resistant concrete," *Journal of Materials in Civil Engineering*, V. 14, No. 3, 2002, pp. 274-7. https://doi.org/10.1061/(ASCE)0899-1561(2002)14:3(27

31. Hadchiti, K., and Carrasquillo, R., "Abrasion resistance and scaling resistance of concrete containing fly ash," *Texas Department of Transportation*, Interim Report (FHWA/TX-89+481-3), 1988, 216 pp.

32. Kevern, J. T., Schaefer, V. R., and Wang, K., "The effect of curing regime on pervious concrete abrasion resistance," *Journal of Testing and Evaluation*, V. 37, No. 4, 2009, pp. 337-42. 10.1520/JTE101761

33. Fentress, B., "Slab construction practices compared by wear tests," *ACI Committee 302 Symposium*, V. 70, 1973, pp. 486-93. 10.14359/11227

34. Sadegzadeh, M., Page, C., and Kettle, R., "Surface microstructure and abrasion resistance of concrete," *Cement and Concrete Research*, V. 17, No. 4, 1987, pp. 581-90. https://doi.org/10.1016/0008-8846(87)90131-1

35. Kilic, A., Atis, C., Teymen, A., Karahan, O., Ozcan, F., and Bilim, C., et al., "The influence of aggregate type on the strength and abrasion resistance of high strength concrete," *Cement and Concrete Composites*, V. 30, No. 4, 2008, pp. 290-6. https://doi.org/10.1016/j.cemconcomp.2007.05.011

36. Naik, T. R., Singh, S. S., and Hossain, M. M., "Abrasion resistance of high-strength concrete made with class C fly ash," *ACI Materials Journal*, V. 92, No. 6, 1995, pp. 649-59. 10.14359/9785

37. Bakke, K. J., "Abrasion resistance," *ASTM International*, STP37736S, Chapter 18, 2006, pp. 184–93. 10.1520/STP37736S

38. Scholz, T. V., and Keshari, S., "Abrasion-resistant concrete mix designs for precast bridge deck panels," *Oregon Department of Transportation*, Report Number: FHWA-OR-RD-11-04, 2010, 91 pp. https://rosap.ntl.bts.gov/view/dot/18287

39. ASTM C418-20, "Standard Test Method for Abrasion Resistance of Concrete by Sandblasting," ASTM International, West Conshohocken, PA, 2020, 4 pp.

40. ASTM C944-19, "Standard Test Method for Abrasion Resistance of Concrete or Mortar Surfaces by the Rotating-Cutter Method," ASTM International, West Conshohocken, PA, 2019, 5 pp.

41. ASTM C779-19, "Standard Test Method for Abrasion Resistance of Horizontal Concrete Surfaces," ASTM International, West Conshohocken, PA, 2019, 5 pp.

42. ASTM C1803-23, "Standard Guide for Abrasion Resistance of Mortar Surfaces Using a Rotary Platform Abraser," ASTM International, West Conshohocken, PA, 2023, 6 pp.

43. IS 9284, "Method of test for abrasion resistance of concrete," Bureau of Indian Standards, 1979.

44. CSA A23.1 A23.2, "Concrete materials and methods of concrete construction/test methods and standard practices for concrete," Canadian Standards Association, 2024, 933 pp.

45. GB/T 16925-1997, "Test method for abrasion resistance of concrete and its products (Ball bearing method)," State Bureau of Technical Supervision, 1998.

46. BS EN 13892-4:2002 "Methods of test for screed materials - Determination of wear resistance-BCA," British Standards Institution, UK, 2002.

47. BS 8204-2:2003+A2:2011, "Screeds, bases and in-situ floorings - Concrete wearing surfaces. Code of practice," British Standards Institution, UK, 2003.

48. Sadezadeh, M., and Kettle, R., "Indirect and non-destructive methods for assessing abrasion resistance of concrete," *Magazine of Concrete Research*, V. 38, No. 137, 1986, pp. 183-90.

49. Meza, A., Ortiz, J., Peralta, L., and Sánchez, C., "Comparison between destructive and nondestructive tests in the evaluation of abrasion resistance of concrete," *Journal of Testing and Evaluation*, V. 46, No. 3, 2018, pp. 906-12.

50. Witzke, F. B., Beltrame, N. A. M., da Luz, C. A., and Medeiros-Junior, R. A., "Abrasive wear of concrete measured by different accelerated tests and natural exposure," *Wear*, V. 520, 2023, pp. 204655.

51. ASTM C31-23, "Standard Practice for Making and Curing Concrete Test Specimens in the Field," ASTM International, West Conshohocken, PA, 2023, 7 pp.

52. ASTM C33-24a, "Standard Specification for Concrete Aggregates," ASTM International, West Conshohocken, PA, 2024, 7 pp.

53. ASTM C39-24, "Standard Test Method for Compressive Strength of Cylindrical Concrete Specimens," ASTM International, West Conshohocken, PA, 2024, 6 pp.

54. Fahim, A., Admassu, N., Dailey, G., and Khanzadeh Moradllo, M., "Application of cellulose nanocrystals in 3D printed alkali-activated cementitious composites," *Journal of Building Engineering*, V. 82, 2024, pp. 108380.

55. Bardestani, R., Patience, G. S., and Kaliaguine, S., "Experimental methods in chemical engineering: specific surface area and pore size distribution measurements—BET, BJH, and DFT," *The Canadian Journal of Chemical Engineering*, V. 97, No. 11, 2019, pp. 2781-91. https://doi.org/10.1002/cjce.23632

56. Fahim, A., and Khanzadeh Moradllo, M., "Unlocking the Depth-Dependent Limitation of External CO_2 Curing in Carbonatable Cementitious Materials Using Enzymatic Solution-Impregnated Hydrogels," *ACS Sustainable Chemistry & Engineering*, V. 13, No. 7, 2025, PP. 2805–2817. https://doi.org/10.1021/acssuschemeng.4c08707

57. Naderi, M., "Surface area: brunauer–emmett–teller (BET)," *Elsevier*, 2015, pp. 585-608.

58. Moon, G. D., Oh, S., Jung, S. H., and Choi, Y. C., "Effects of the fineness of limestone powder and cement on the hydration and strength development of PLC concrete," *Construction and Building Materials*, V. 135, 2017, pp. 129-36. https://doi.org/10.1016/j.conbuildmat.2016.12.189

59. Aranda, M. A., Artioli, I., Bier, T., Àngeles, G., Freyer, D., and Kaden, R., et al., "Cementitious materials: Composition, properties, application." *Walter de Gruyter GmbH & Co KG*; 2017. https://doi.org/10.1515/9783110473728

60. Gartner, E., Young, J., Damidot, D., Jawed, I., "Hydration of Portland cement," *Structure and Performance of Cements*, V. 2, 2002, pp. 57-113.

61. Scrivener, K.L., Juilland, P., and Monteiro, P.J., "Advances in understanding hydration of Portland cement," *Cement and Concrete Research*, V. 78. 2015, pp. 38-56. https://doi.org/10.1016/j.cemconres.2015.05.025.

62. Sonebi, M., and Khayat, K., "Testing abrasion resistance of high-strength concrete," *Cement, Concrete, and Aggregates*, V. 23, No. 1, 2001, pp. 34-43. https://doi.org/10.1520/CCA10523J

63. Pyo, S., Abate, S.Y., and Kim, H.-K., "Abrasion resistance of ultra-high-performance concrete incorporating coarser aggregate," *Construction and Building Materials*, V. 165. 2018, pp. 11-6. https://doi.org/10.1016/j.conbuildmat.2018.01.036.

64. L. Shuhua, H. Weiwei, L. Qiaol, "Hydration properties of ground granulated blast-furnace slag (GGBS) under different hydration environments," *Materials Science* 23(1) (2017) 70-77 DOI: http://dx.doi.org/10.5755/j01.ms.23.1.14878.

65. Y. Briki, M. Zajac, M.B. Haha, K. Scrivener, "Factors affecting the reactivity of slag at early and late ages," *Cement and Concrete Research* 150 (2021) 106604 DOI: https://doi.org/10.1016/j.cemconres.2021.106604.

66. Y. Zhang, S. Zhang, Y. Chen, O. Çopuroğlu, "The effect of slag chemistry on the reactivity of synthetic and commercial slags," *Construction and Building Materials* 335 (2022) 127493 DOI: https://doi.org/10.1016/j.conbuildmat.2022.127493.